

**INTERPRETATION REPORT ON A HELICOPTER-BORNE
VERSATILE TIME DOMAIN ELECTROMAGNETIC (VTEM^{plus}) AND
HORIZONTAL MAGNETIC GRADIOMETER GEOPHYSICAL SURVEY**



**Dinty Lake Property Area
Stony Rapids, Saskatchewan, Canada**

**For:
Canexplor Management Ltd.**

**By:
Aeroquest Airborne
7687 Bath Road
Mississauga, ON, CANADA, L4T 3T1
Tel: 1.905.672.9129
Fax: 1.905.672.7083
www.aeroquestairborne.com
Email: sales@aeroquestairborne.com**

Survey flown during April 2013

Project AQ130191

June, 2013

TABLE OF CONTENTS

EXECUTIVE SUMMARY	iii
1. INTRODUCTION.....	1
1.1 General Considerations	1
1.2 Survey and System Specifications	2
1.3 Topographic Relief and Cultural Features	3
2. DATA ACQUISITION	4
2.1 Survey Area	4
2.2 Survey Operations	4
2.3 Flight Specifications	5
2.4 Aircraft and Equipment.....	5
2.4.1 Survey Aircraft.....	5
2.4.2 Electromagnetic System	5
2.4.3 Horizontal Magnetic Gradiometer.....	8
2.4.4 Radar Altimeter	8
2.4.5 GPS Navigation System.....	8
2.4.6 Digital Acquisition System.....	8
2.5 Base Station.....	9
3. PERSONNEL	10
4. DATA PROCESSING AND PRESENTATION	11
4.1 Flight Path.....	11
4.2 Electromagnetic Data.....	11
4.3 Horizontal Magnetic Gradiometer Data.....	13
5. DELIVERABLES.....	14
5.1 Survey Report	14
5.2 Digital Data.....	14
6. INTERPRETATION SUMMARY	19
6.1 Geological Setting.....	19
6.2 Tau Parameters and CVG Calculation.....	19
6.3 Resistivity Depth Imaging.....	20
6.4 Identification of Anomalous Zones.....	21
7. CONCLUSIONS AND RECOMMENDATIONS.....	25

LIST OF FIGURES

Figure 1: Property Location.....	1
Figure 2: Survey area location on Google Earth.....	2
Figure 3: Flight path over a Google Earth Image.....	3
Figure 4: VTEM Waveform & Sample Times.....	5
Figure 5: VTEMplus System Configuration.....	7
Figure 6: Z, X and Fraser filtered X (FFx) components for “thin” target.....	12
Figure 7 – Image of Time Constant (Tau, dBz/dt) and Calculated Vertical Gradient (CVG) of TMI contours, highlighting flight path of RDIs – Dinty Lake property	20
Figure 8 – Resistivity Depth Image (RDI) of L3100, anomaly D1 – Dinty Lake property	21
Figure 9 – Tau image and CVG contours of TMI, highlighting conductive anomalies and magnetic lineaments (black arrow) that cross-cut where anomalous zone D2 is identified – Dinty Lake property	22
Figure 10 – Resistivity Depth Image (RDI) of L3410, anomalous Zone D3 – Dinty Lake Property.....	23
Figure 11 – VTEM profiles of dBz/dt overlaying the magnetic Tilt derivative (rendering transparency) and recommended anomalous zones (D1, D2, D3) to follow-up – Dinty Lake property	24
Figure 12 – Tau dB/dt Z over CVG contours showing the anomalous zones	25

LIST OF TABLES

Table 1: Survey Specifications.....	4
Table 2: Survey schedule	4
Table 3: Off-Time Decay Sampling Scheme.....	6
Table 4: Acquisition Sampling Rates	8
Table 5: Geosoft GDB Data Format.....	15
Table 6: Geosoft Resistivity Depth Image GDB Data Format.....	16

APPENDICES

A. Survey location maps	
B. Survey Block Coordinates	
C. Geophysical Maps	
D. Generalized Modelling Results of the VTEM System	
E. TAU Analysis	
F. TEM Resistivity Depth Imaging (RDI)	

REPORT ON A HELICOPTER-BORNE VERSATILE TIME DOMAIN ELECTROMAGNETIC (VTEM^{plus}) and HORIZONTAL MAGNETIC GRADIOMETER GEOPHYSICAL SURVEY

Dinty Lake Property Area
Stony Rapids, Saskatchewan, Canada

EXECUTIVE SUMMARY

On April 24th, 2013 Aeroquest Airborne carried out a helicopter-borne geophysical survey over the Dinty Lake property area situated near Stony Rapids, Saskatchewan, Canada.

Principal geophysical sensors included a versatile time domain electromagnetic (VTEM^{plus}) system, and horizontal magnetic gradiometer. Ancillary equipment included a GPS navigation system and a radar altimeter. A total of 158 line-kilometres of geophysical data were acquired during the survey.

In-field data quality assurance and preliminary processing were carried out on a daily basis during the acquisition phase. Preliminary and final data processing, including generation of final digital data and map products were undertaken from the office of Geotech Ltd. in Aurora, Ontario.

The processed survey results are presented as the following maps:

- Electromagnetic stacked profiles of the B-field Z Component,
- Electromagnetic stacked profiles of dB/dt Z Components,
- B-Field Z Component Channel grid
- Fraser Filtered dB/dt X Component Channel grid
- Total Magnetic Intensity (TMI),
- Magnetic Total Horizontal Gradient
- Magnetic Tilt-Angle Derivative
- Calculated Time Constant (Tau) with contours of anomaly areas of the Calculated Vertical Derivative of TMI
- RDI sections are presented.

Digital data includes all electromagnetic and magnetic products, plus ancillary data including the waveform.

The survey report describes the procedures for data acquisition, processing, final image presentation and the specifications for the digital data set.

1. INTRODUCTION

1.1 General Considerations

Aeroquest Airborne performed a helicopter-borne geophysical survey over the Dinty Lake property area located near Stony Rapids, Saskatchewan, Canada (Figure 1 & 2).

Reza Mohammed represented Canexplor Management Ltd. during the data acquisition and data processing phases of this project.

The geophysical surveys consisted of helicopter borne EM using the versatile time-domain electromagnetic (VTEM^{plus}) system with Z and X component measurements and horizontal magnetic gradiometer using two cesium magnetometers. A total of 158 line-km of geophysical data were acquired during the survey.

The crew was based out of Stony Rapids (Figure 2) in Saskatchewan for the acquisition phase of the survey. Survey flying was started on April 24th, 2013 and completed on April 27th, 2013.

Data quality control and quality assurance, and preliminary data processing were carried out on a daily basis during the acquisition phase of the project. Final data processing followed immediately after the end of the survey. Final reporting, data presentation and archiving were completed from the Aurora office of Geotech Ltd. in June, 2013.

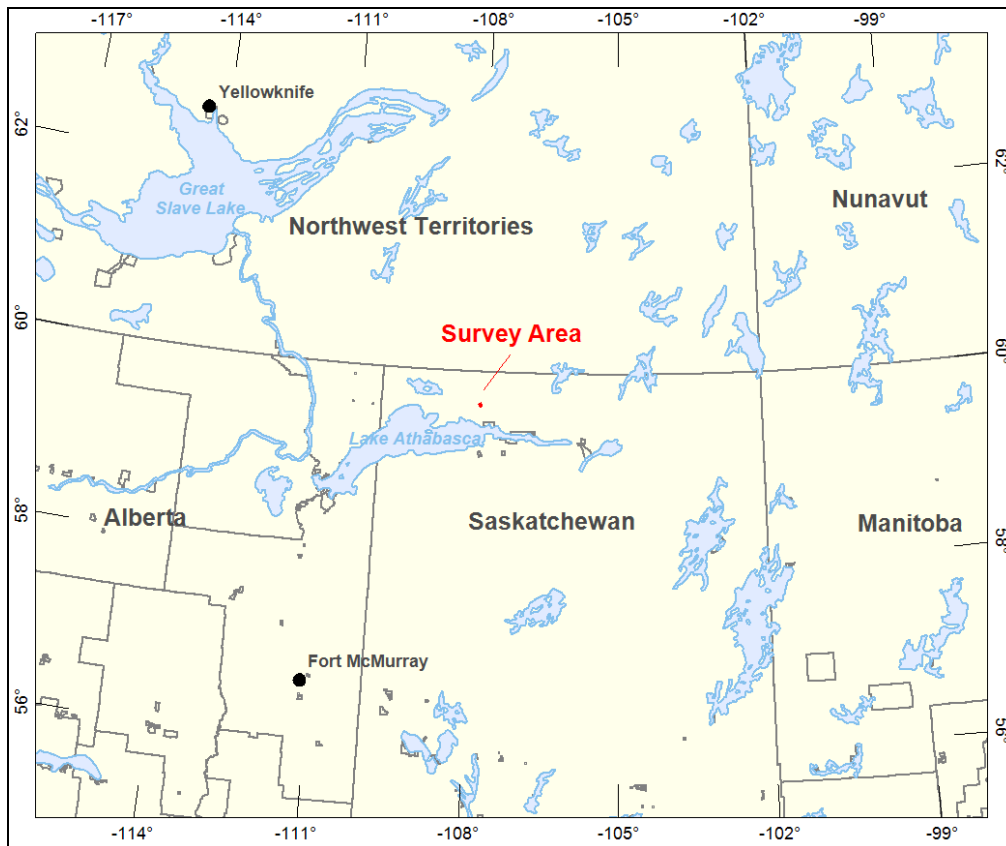


Figure 1: Property Location.

1.2 Survey and System Specifications

The survey area is located in close proximity to Stony Rapids, Saskatchewan, Canada (Figure 2).



Figure 2: Survey area location on Google Earth.

The Dinty property was flown in a northwest to southeast ($N 64^\circ$ azimuth) direction with traverse line spacing of 100 metres as depicted in Figure 4. Tie lines were flown perpendicular to the traverse lines at a spacing of 1000 metres respectively. For more detailed information on the flight spacing and direction see Table 1.

1.3 Topographic Relief and Cultural Features

Dinty Property

Topographically, the block exhibits a shallow relief with an elevation ranging from 356 to 451 metres above mean sea level over an area of 15 square kilometres (Figure 3).

There are various rivers and streams running through the survey area which connect various lakes and wetlands. There are no visible signs of culture which run throughout the survey area.

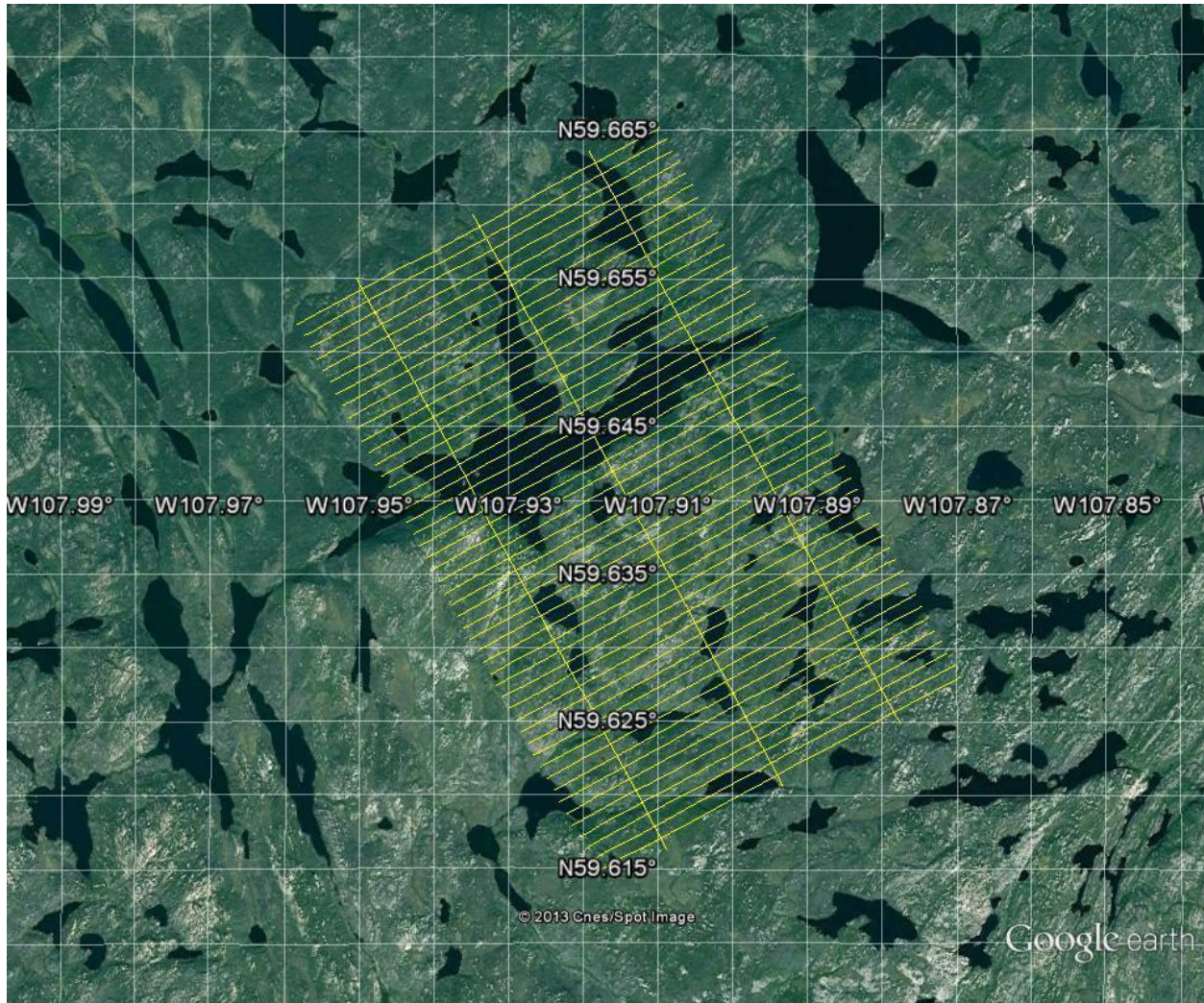


Figure 3: Flight path over a Google Earth Image.

The survey area is covered by numerous mining claims, which are plotted on all maps. The survey area is covered by NTS (National Topographic Survey) of Canada sheets 074012.

2. DATA ACQUISITION

2.1 Survey Area

The survey block (see Figure 3 and Appendix A) and general flight specifications are as follows:

Table 1: Survey Specifications

Survey block	Traverse Line spacing (m)	Area (Km ²)	Planned Line-km ¹	Actual Line-km	Flight direction	Line numbers
Dinty	Traverse: 100	15	158	164	N 64° E / N 244° E	L3000-L3470
	Tie: 1000				N 154° E / N 334° E	T3800-T3820
TOTAL		15	158	164		

Survey block boundaries co-ordinates are provided in Appendix B.

2.2 Survey Operations

Survey operations were based out of Stony Rapids in Saskatchewan on April 24th, 2013. The following table shows the timing of the flying.

Table 2: Survey schedule

Date	Flight #	Flow km	Block	Crew location	Comments
24-Apr-2013				Stony Rapids SK	mobilization
25-Apr-2013				Stony Rapids SK	Crew arrived
26-Apr-2013	1,2,3	329	Dinty W&E	Stony Rapids SK	329km flown
27-Apr-2013	4	45	E	Stony Rapids SK	Remaining kms were flown – flying complete
				Stony Rapids SK	

¹ Note: Actual Line kilometres represent the total line kilometres in the final database. These line-km normally exceed the planned line-km, as indicated in the survey NAV files.

2.3 Flight Specifications

During the survey the helicopter was maintained at a mean altitude of 75 metres above the ground with an average survey speed of 80 km/hour. This allowed for an actual average EM bird terrain clearance of 41 metres and a magnetic sensor clearance of 51 metres.

The on board operator was responsible for monitoring the system integrity. He also maintained a detailed flight log during the survey, tracking the times of the flight as well as any unusual geophysical or topographic features.

On return of the aircrew to the base camp the survey data was transferred from a compact flash card (PCMCIA) to the data processing computer. The data were then uploaded via ftp to the Geotech office in Aurora for daily quality assurance and quality control by qualified personnel.

2.4 Aircraft and Equipment

2.4.1 Survey Aircraft

The survey was flown using a Eurocopter Aerospatiale (Astar) 350 B3 helicopter, registration C-FK0I. The helicopter is owned and operated by Geotech Aviation. Installation of the geophysical and ancillary equipment was carried out by a Geotech Ltd crew.

2.4.2 Electromagnetic System

The electromagnetic system was a Geotech Time Domain EM (VTEM^{plus}) system. VTEM with the Serial number 8 had been used for the survey. The configuration is as indicated in Figure 5.

The VTEM Receiver and transmitter coils were in concentric-coplanar and Z-direction oriented configuration. The receiver system for the project also included a coincident-coaxial X-direction coil to measure the in-line dB/dt and calculate B-Field responses. The EM bird was towed at a mean distance of 34 metres below the aircraft as shown in Figure 5. The receiver decay recording scheme is shown diagrammatically in Figure 4.

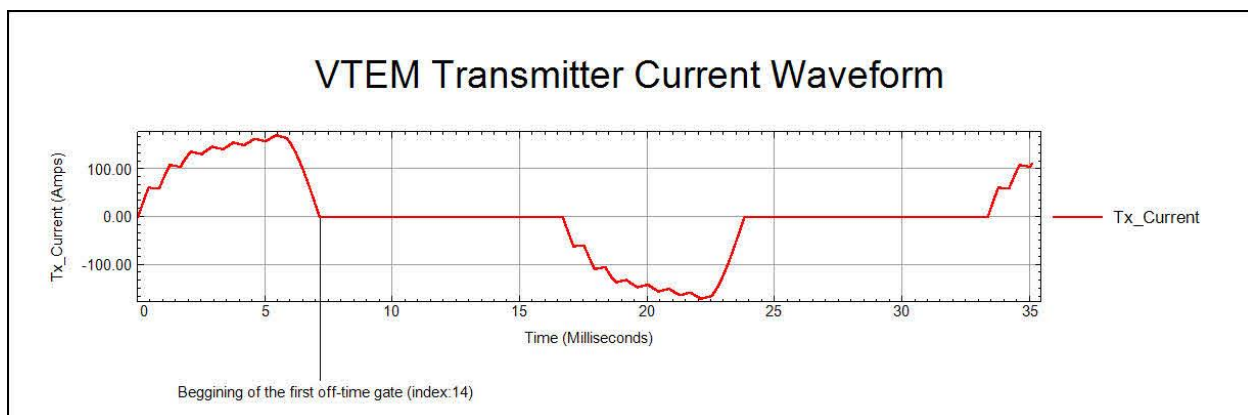


Figure 4: VTEM Waveform & Sample Times.

The VTEM decay sampling scheme is shown in Table 3 below. Thirty-two time measurement gates were used for the final data processing in the range from 0.096 to 7.036 msec.

Table 3: Off-Time Decay Sampling Scheme

VTEM Decay Sampling Scheme			
Index	Middle	Start	End
Milliseconds			
14	0.096	0.090	0.103
15	0.110	0.103	0.118
16	0.126	0.118	0.136
17	0.145	0.136	0.156
18	0.167	0.156	0.179
19	0.192	0.179	0.206
20	0.220	0.206	0.236
21	0.253	0.236	0.271
22	0.290	0.271	0.312
23	0.333	0.312	0.358
24	0.383	0.358	0.411
25	0.440	0.411	0.472
26	0.505	0.472	0.543
27	0.580	0.543	0.623
28	0.667	0.623	0.716
29	0.766	0.716	0.823
30	0.880	0.823	0.945
31	1.010	0.945	1.086
32	1.161	1.086	1.247
33	1.333	1.247	1.432
34	1.531	1.432	1.646
35	1.760	1.646	1.891
36	2.021	1.891	2.172
37	2.323	2.172	2.495
38	2.667	2.495	2.865
39	3.063	2.865	3.292
40	3.521	3.292	3.781
41	4.042	3.781	4.341
42	4.641	4.341	4.987
43	5.333	4.987	5.729
44	6.125	5.729	6.581
45	7.036	6.581	7.560

Z Component: 14-45 time gates
X Component: 20-45 time gates.

VTEM system specifications:

Transmitter

- Transmitter coil diameter: 26 m
- Number of turns: 4
- Effective Transmitter coil area: 2123.7 m²
- Transmitter base frequency: 30 Hz
- Peak current: 173 A
- Pulse width: 7.15 ms
- Wave form shape: Bi-polar trapezoid
- Peak dipole moment: 367,402 nA
- Actual average EM Bird terrain clearance: 41 metres above the ground

Receiver

- X Coil diameter: 0.32 m
- Number of turns: 245
- Effective coil area: 19.69 m²
- Z-Coil coil diameter: 1.2 m
- Number of turns: 100
- Effective coil area: 113.04 m²

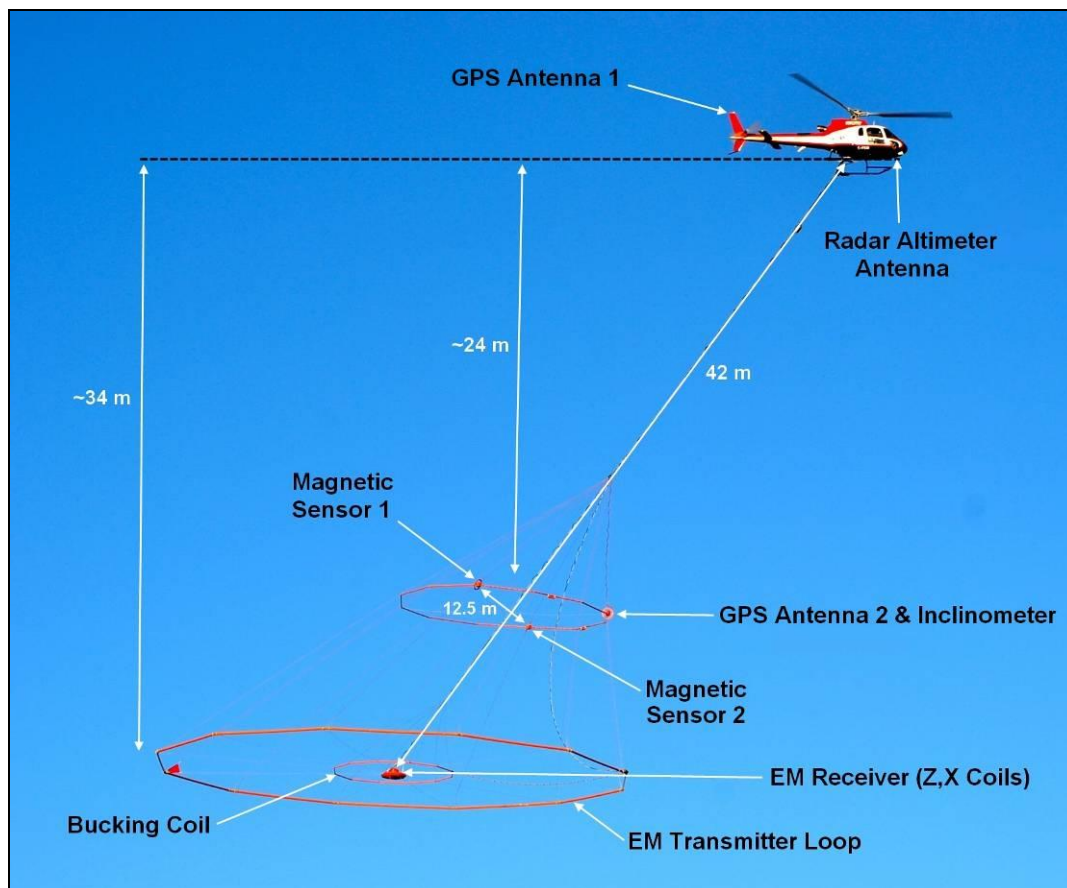


Figure 5: VTEM^{plus} System Configuration.

2.4.3 Horizontal Magnetic Gradiometer

The horizontal magnetic gradiometer consists of two Geometrics split-beam field magnetic sensors with a sampling interval of 0.1 seconds. These sensors are mounted 12.5 metres apart on a separate loop, 10 metres above the EM bird. A GPS antenna and Gyro Inclinator is installed on the separate loop to accurately record the tilt and position of the magnetic gradiometer bird.

2.4.4 Radar Altimeter

A Terra TRA 3000/TRI 40 radar altimeter was used to record terrain clearance. The antenna was mounted beneath the bubble of the helicopter cockpit (Figure 5).

2.4.5 GPS Navigation System

The navigation system used was a Geotech PC104 based navigation system utilizing a NovAtel's WAAS (Wide Area Augmentation System) enabled GPS receiver, Geotech navigate software, a full screen display with controls in front of the pilot to direct the flight and a NovAtel GPS antenna mounted on the helicopter tail (Figure 5). As many as 11 GPS and two WAAS satellites may be monitored at any one time. The positional accuracy or circular error probability (CEP) is 1.8 m, with WAAS active, it is 1.0 m. The co-ordinates of the block were set-up prior to the survey and the information was fed into the airborne navigation system. The second GPS antenna is installed on the additional magnetic loop together with Gyro Inclinator.

2.4.6 Digital Acquisition System

A Geotech data acquisition system recorded the digital survey data on an internal compact flash card. Data is displayed on an LCD screen as traces to allow the operator to monitor the integrity of the system. The data type and sampling interval as provided in Table 4.

Table 4: Acquisition Sampling Rates

Data Type	Sampling
TDEM	0.1 sec
Magnetometer	0.1 sec
GPS Position	0.2 sec
Radar Altimeter	0.2 sec
Inclinometer	0.1 sec

2.5 Base Station

A combined magnetometer/GPS base station was utilized on this project. A Geometrics Cesium vapour magnetometer was used as a magnetic sensor with a sensitivity of 0.001 nT. The base station was recording the magnetic field together with the GPS time at 1 Hz on a base station computer.

The base station magnetometer sensor was installed behind a cabin next to the shoreline (59°15.3754N, 105°50.3728W); away from electric transmission lines and moving ferrous objects such as motor vehicles. The base station data were backed-up to the data processing computer at the end of each survey day.

3. PERSONNEL

The following Geotech Ltd. personnel were involved in the project.

Field:

Project Manager:	Scott Trew (Office)
Data QC:	Neil Fiset (Office)
Crew chief:	Joseph Florjancic
Operator:	Jan Dabrowski

The survey pilot and the mechanical engineer were employed directly by the helicopter operator – Geotech Aviation.

Pilot:	Claude Noel
Mechanical Engineer:	N/A

Office:

Preliminary Data Processing:	Neil Fiset Thomas Wade
Final Data Processing:	Keeme Mokubung
Final Data QA/QC:	Alexander Prikhodko
Reporting/Mapping:	Karl Monje

Data acquisition phase was carried out under the supervision of Andrei Bagrianski, P. Geo, Chief Operating Officer. Processing and Interpretation phases were carried out under the supervision of Alexander Prikhodko, P. Geo, Senior Geophysicist, VTEM Interpretation Supervisor. The customer relations were looked after by Paolo Berardelli.

4. DATA PROCESSING AND PRESENTATION

Data compilation and processing were carried out by the application of Geosoft OASIS Montaj and programs proprietary to Geotech Ltd.

4.1 Flight Path

The flight path, recorded by the acquisition program as WGS 84 latitude/longitude, was converted into the NAD83 Datum, UTM Zone 13 North coordinate system in Oasis Montaj.

The flight path was drawn using linear interpolation between x, y positions from the navigation system. Positions are updated every second and expressed as UTM easting's (x) and UTM northing's (y).

4.2 Electromagnetic Data

A three stage digital filtering process was used to reject major spheric events and to reduce noise levels. Local spheric activity can produce sharp, large amplitude events that cannot be removed by conventional filtering procedures. Smoothing or stacking will reduce their amplitude but leave a broader residual response that can be confused with geological phenomena. To avoid this possibility, a computer algorithm searches out and rejects the major spheric events.

The signal to noise ratio was further improved by the application of a low pass linear digital filter. This filter has zero phase shift which prevents any lag or peak displacement from occurring, and it suppresses only variations with a wavelength less than about 1 second or 15 metres. This filter is a symmetrical 1 sec linear filter.

The results are presented as stacked profiles of EM voltages for the time gates, in linear - logarithmic scale for the B-field Z component and dB/dt responses in the Z and X components. B-field Z component time channel recorded at 2.021 milliseconds after the termination of the impulse is also presented as a colour image. Calculated Time Constant (TAU) with anomaly contours of Calculated Vertical Derivative of TMI is presented in Appendix C and E. Resistivity Depth Image (RDI) is also presented in Appendix E and F.

VTEM has two receiver coil orientations. Z-axis coil is oriented parallel to the transmitter coil axis and both are horizontal to the ground. The X-axis coil is oriented parallel to the ground and along the line-of-flight. This combined two coil configuration provides information on the position, depth, dip and thickness of a conductor. Generalized modeling results of VTEM data, are shown in Appendix D.

In general X-component data produce cross-over type anomalies: from "+ to -" in flight direction of flight for "thin" sub vertical targets and from "- to +" in direction of flight for "thick" targets. Z component data produce double peak type anomalies for "thin" sub vertical targets and single peak for "thick" targets.

The limits and change-over of "thin-thick" depends on dimensions of a TEM system (Appendix D, Figure D-16).

Because of X component polarity is under line-of-flight, convolution Fraser Filter (Figure 6) is applied to X component data to represent axes of conductors in the form of grid map. In this case positive FF anomalies always correspond to “plus-to-minus” X data crossovers independent of the flight direction.

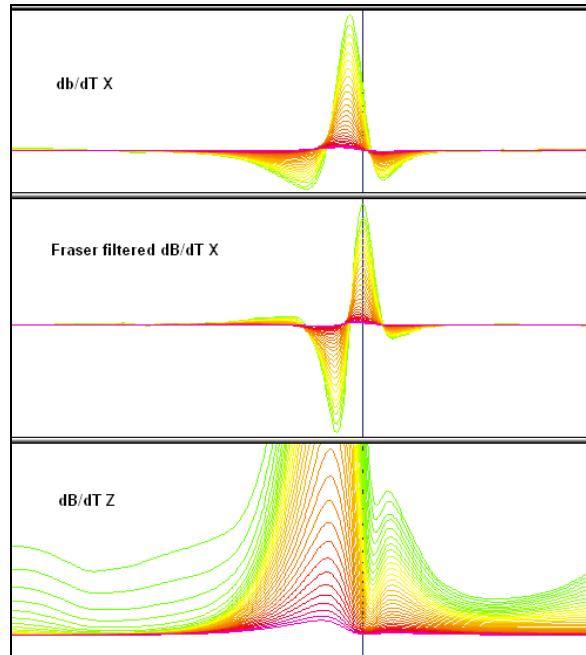


Figure 6: Z, X and Fraser filtered X (FFx) components for “thin” target.

4.3 Horizontal Magnetic Gradiometer Data

The horizontal gradients data from the VTEM^{plus} are measured by two magnetometers 12.5 m apart on an independent bird mounted 10m above the VTEM loop. A GPS and a Gyro Inclinometer help to determine the positions and orientations of the magnetometers. The data from the two magnetometers are corrected for position and orientation variations, as well as for the diurnal variations using the base station data.

The position of the centre of the horizontal magnetic gradiometer bird is calculated from the GPS utilizing in-house processing tool in Geosoft. Following that total magnetic intensity is calculated at the center of the bird by calculating the mean values from both sensors. In addition to the total intensity advanced processing is done to calculate the in-line and cross-line (or lateral) horizontal gradient which enhance the understanding of magnetic targets. The in-line (longitudinal) horizontal gradient is calculated from the difference of two consecutive total magnetic field readings divided by the distance along the flight line direction, while the cross-line (lateral) horizontal magnetic gradient is calculated from the difference in the magnetic readings from both magnetic sensors divided by their horizontal separation.

Two advanced magnetic derivative products, the total horizontal derivative (THDR), and tilt angle derivative and are also created. The total horizontal derivative or gradient is also called the analytic signal, is defined as:

$THDR = \sqrt{H_x^2 + H_y^2}$, where H_x and H_y are cross-line and in-line horizontal gradients.

The tilt angle derivative (TDR) is defined as:

$TDR = \arctan(V_z / THDR)$, where THDR is the total horizontal derivative, and V_z is the vertical derivative.

Measured cross-line gradients can help to enhance cross-line linear features during gridding.

5. DELIVERABLES

5.1 Survey Report

The survey report describes the data acquisition, processing, and final presentation of the survey results. The survey report is provided in two paper copies and digitally in PDF format.

5.2 Digital Data

Two copies of the data and maps on DVD were prepared to accompany the report. Each DVD contains a digital file of the line data in GDB Geosoft Montaj format as well as the maps in Geosoft Montaj Map and PDF format.

- DVD structure.

Data	contains databases, grids and maps, as described below.
Report	contains a copy of the report and appendices in PDF format.

Databases in Geosoft GDB format, containing the channels listed in Table 5.

Table 5: Geosoft GDB Data Format

Channel name	Units	Description
X:	metres	UTM Easting NAD83 Zone 13 North
Y:	metres	UTM Northing NAD83 Zone 13 North
Longitude:	Decimal Degrees	WGS 84 Longitude data
Latitude:	Decimal Degrees	WGS 84 Latitude data
Z:	metres	GPS antenna elevation (above Geoid)
Radar:	metres	helicopter terrain clearance from radar altimeter
Radarb:	metres	Calculated EM bird terrain clearance from radar altimeter
DEM:	metres	Digital Elevation Model
Gtime:	Seconds of the day	GPS time
Mag1L:	nT	Measured Total Magnetic field data (left sensor)
Mag1R:	nT	Measured Total Magnetic field data (right sensor)
Basemag:	nT	Magnetic diurnal variation data
Mag2LZ	nT	Z corrected (w.r.t. loop center) and diurnal corrected magnetic field left mag
Mag2RZ	nT	Z corrected (w.r.t. loop center) and diurnal corrected magnetic field right mag
TMI2	nT	Calculated from diurnal corrected total magnetic field intensity of the centre of the loop
TMI3	nT	Microleveled total magnetic field intensity of the centre of the loop
Hgcxline		measured cross-line gradient
Hginline		Calculated in-line gradient
CVG	nT/m	Calculated Magnetic Vertical Gradient
SFz[14]:	pV/(A*m ⁴)	Z dB/dt 0.096 millisecond time channel
SFz[15]:	pV/(A*m ⁴)	Z dB/dt 0.110 millisecond time channel
SFz[16]:	pV/(A*m ⁴)	Z dB/dt 0.126 millisecond time channel
SFz[17]:	pV/(A*m ⁴)	Z dB/dt 0.145 millisecond time channel
SFz[18]:	pV/(A*m ⁴)	Z dB/dt 0.167 millisecond time channel
SFz[19]:	pV/(A*m ⁴)	Z dB/dt 0.192 millisecond time channel
SFz[20]:	pV/(A*m ⁴)	Z dB/dt 0.220 millisecond time channel
SFz[21]:	pV/(A*m ⁴)	Z dB/dt 0.253 millisecond time channel
SFz[22]:	pV/(A*m ⁴)	Z dB/dt 0.290 millisecond time channel
SFz[23]:	pV/(A*m ⁴)	Z dB/dt 0.333 millisecond time channel
SFz[24]:	pV/(A*m ⁴)	Z dB/dt 0.383 millisecond time channel
SFz[25]:	pV/(A*m ⁴)	Z dB/dt 0.440 millisecond time channel
SFz[26]:	pV/(A*m ⁴)	Z dB/dt 0.505 millisecond time channel
SFz[27]:	pV/(A*m ⁴)	Z dB/dt 0.580 millisecond time channel
SFz[28]:	pV/(A*m ⁴)	Z dB/dt 0.667 millisecond time channel
SFz[29]:	pV/(A*m ⁴)	Z dB/dt 0.766 millisecond time channel
SFz[30]:	pV/(A*m ⁴)	Z dB/dt 0.880 millisecond time channel
SFz[31]:	pV/(A*m ⁴)	Z dB/dt 1.010 millisecond time channel
SFz[32]:	pV/(A*m ⁴)	Z dB/dt 1.161 millisecond time channel
SFz[33]:	pV/(A*m ⁴)	Z dB/dt 1.333 millisecond time channel
SFz[34]:	pV/(A*m ⁴)	Z dB/dt 1.531 millisecond time channel
SFz[35]:	pV/(A*m ⁴)	Z dB/dt 1.760 millisecond time channel
SFz[36]:	pV/(A*m ⁴)	Z dB/dt 2.021 millisecond time channel
SFz[37]:	pV/(A*m ⁴)	Z dB/dt 2.323 millisecond time channel
SFz[38]:	pV/(A*m ⁴)	Z dB/dt 2.667 millisecond time channel
SFz[39]:	pV/(A*m ⁴)	Z dB/dt 3.063 millisecond time channel
SFz[40]:	pV/(A*m ⁴)	Z dB/dt 3.521 millisecond time channel
SFz[41]:	pV/(A*m ⁴)	Z dB/dt 4.042 millisecond time channel

Channel name	Units	Description
SFz[42]:	$\text{pV}/(\text{A}^*\text{m}^4)$	Z dB/dt 4.641 millisecond time channel
SFz[43]:	$\text{pV}/(\text{A}^*\text{m}^4)$	Z dB/dt 5.333 millisecond time channel
SFz[44]:	$\text{pV}/(\text{A}^*\text{m}^4)$	Z dB/dt 6.125 millisecond time channel
SFz[45]:	$\text{pV}/(\text{A}^*\text{m}^4)$	Z dB/dt 7.036 millisecond time channel
SFx[20]:	$\text{pV}/(\text{A}^*\text{m}^4)$	X dB/dt 0.220 millisecond time channel
SFx[21]:	$\text{pV}/(\text{A}^*\text{m}^4)$	X dB/dt 0.253 millisecond time channel
SFx[22]:	$\text{pV}/(\text{A}^*\text{m}^4)$	X dB/dt 0.290 millisecond time channel
SFx[23]:	$\text{pV}/(\text{A}^*\text{m}^4)$	X dB/dt 0.333 millisecond time channel
SFx[24]:	$\text{pV}/(\text{A}^*\text{m}^4)$	X dB/dt 0.383 millisecond time channel
SFx[25]:	$\text{pV}/(\text{A}^*\text{m}^4)$	X dB/dt 0.440 millisecond time channel
SFx[26]:	$\text{pV}/(\text{A}^*\text{m}^4)$	X dB/dt 0.505 millisecond time channel
SFx[27]:	$\text{pV}/(\text{A}^*\text{m}^4)$	X dB/dt 0.580 millisecond time channel
SFx[28]:	$\text{pV}/(\text{A}^*\text{m}^4)$	X dB/dt 0.667 millisecond time channel
SFx[29]:	$\text{pV}/(\text{A}^*\text{m}^4)$	X dB/dt 0.766 millisecond time channel
SFx[30]:	$\text{pV}/(\text{A}^*\text{m}^4)$	X dB/dt 0.880 millisecond time channel
SFx[31]:	$\text{pV}/(\text{A}^*\text{m}^4)$	X dB/dt 1.010 millisecond time channel
SFx[32]:	$\text{pV}/(\text{A}^*\text{m}^4)$	X dB/dt 1.161 millisecond time channel
SFx[33]:	$\text{pV}/(\text{A}^*\text{m}^4)$	X dB/dt 1.333 millisecond time channel
SFx[34]:	$\text{pV}/(\text{A}^*\text{m}^4)$	X dB/dt 1.531 millisecond time channel
SFx[35]:	$\text{pV}/(\text{A}^*\text{m}^4)$	X dB/dt 1.760 millisecond time channel
SFx[36]:	$\text{pV}/(\text{A}^*\text{m}^4)$	X dB/dt 2.021 millisecond time channel
SFx[37]:	$\text{pV}/(\text{A}^*\text{m}^4)$	X dB/dt 2.323 millisecond time channel
SFx[38]:	$\text{pV}/(\text{A}^*\text{m}^4)$	X dB/dt 2.667 millisecond time channel
SFx[39]:	$\text{pV}/(\text{A}^*\text{m}^4)$	X dB/dt 3.063 millisecond time channel
SFx[40]:	$\text{pV}/(\text{A}^*\text{m}^4)$	X dB/dt 3.521 millisecond time channel
SFx[41]:	$\text{pV}/(\text{A}^*\text{m}^4)$	X dB/dt 4.042 millisecond time channel
SFx[42]:	$\text{pV}/(\text{A}^*\text{m}^4)$	X dB/dt 4.641 millisecond time channel
SFx[43]:	$\text{pV}/(\text{A}^*\text{m}^4)$	X dB/dt 5.333 millisecond time channel
SFx[44]:	$\text{pV}/(\text{A}^*\text{m}^4)$	X dB/dt 6.125 millisecond time channel
SFx[45]:	$\text{pV}/(\text{A}^*\text{m}^4)$	X dB/dt 7.036 millisecond time channel
BFz	$(\text{pV}*\text{ms})/(\text{A}^*\text{m}^4)$	Z B-Field data for time channels 14 to 45
BFx	$(\text{pV}*\text{ms})/(\text{A}^*\text{m}^4)$	X B-Field data for time channels 20 to 45
SFxFF	$\text{pV}/(\text{A}^*\text{m}^4)$	Fraser Filtered X dB/dt
NchanBF		Latest time channels of TAU calculation
NchanSF		Latest time channels of TAU calculation
TauBF	ms	Time constant B-Field
TauSF	ms	Time constant dB/dt
PLM:		60 Hz power line monitor

Electromagnetic B-field and dB/dt Z component data is found in array channel format between indexes 14 – 45, and X component data from 20 – 45, as described above.

- Database of the Resistivity Depth Images in Geosoft GDB format, containing the following channels:

Table 6: Geosoft Resistivity Depth Image GDB Data Format

Channel name	Units	Description
Xg:	metres	UTM Easting NAD83 Zone 13 North
Yg:	metres	UTM Northing NAD83 Zone 13 North
Dist:	meters	Distance from the beginning of the line
Depth:	meters	array channel, depth from the surface

Channel name	Units	Description
Z:	metres	array channel, depth from sea level
AppRes:	Ohm-m	array channel, Apparent Resistivity
TR:	metres	EM system height from sea level
Topo:	metres	digital elevation model
Radarb:	metres	Calculated EM bird terrain clearance from radar altimeter
Mag:	nT or nT/m	CVG data
SF:	pV/(A*m ⁴)	array channel, dB/dT
DOI	metres	Depth of investigation; a measure of VTEM depth effectiveness

- Database of the VTEM Waveform “AQ130191_Waveform_final.gdb” in Geosoft GDB format, containing the following channels:

Time: Sampling rate interval, 5.2083 milliseconds
Tx_Current: Output current of the transmitter (Amp)
Rx_Volt: Output voltage of the receiver coil (Volt)

- Grids in Geosoft GRD and GeoTIFF format, as follows:

Dinty_BFz36: B-Field Z Component Channel 36 (Time Gate 2.021 ms)
Dinty_CVG: Calculated Magnetic Vertical Gradient (nT/m)
Dinty_DEM: Digital Elevation Model (metres)
Dinty_PLM: Power Line Monitor
Dinty_Hgcxline: Measured Cross-Line Gradient (nT/m)
Dinty_Hginline: Measured In-Line Gradient (nT/m)
Dinty_SFz20: dB/dt Z Component Channel 20 (Time Gate 0.220 ms)
Dinty_SFz30: dB/dt Z Component Channel 30 (Time Gate 0.880 ms)
Dinty_SFz40: dB/dt Z Component Channel 40 (Time Gate 3.521 ms)
Dinty_TauBF: B-Field Z Component, Calculated Time Constant (ms)
Dinty_TauSF: dB/dt Z Component, Calculated Time Constant (ms)
Dinty_TMI3: Total Magnetic Intensity (nT)
Dinty_TotalHGrad: Magnetic Total Horizontal Gradient (nT/m)
Dinty_Tiltdrv: Magnetic Tilt derivative (radians)
Dinty_SFXFF22: Fraser Filtered dB/dt X Component Channel 22 (Time Gate 0.290 ms)

A Geosoft .GRD file has a .GI metadata file associated with it, containing grid projection information. A grid cell size of 25 metres was used.

- Maps at 1:10,000 in Geosoft MAP format, as follows:

JN_20k_BL_dBdt: dB/dt Z Component profiles, Time Gates 0.220 – 7.036 ms in linear – logarithmic scale.
JN_20k_BL_Bfield: B-field Z Component profiles, Time Gates 0.220 – 7.036 ms in linear – logarithmic scale.
JN_20k_BL_BFz36: B-field Z Component Channel 36, Time Gate 2.021 ms colour image.
JN_20K_BL_SFxFF20: Fraser Filtered dB/dt X Component Channel 20, Time Gate 0.220 ms colour image.
JN_20k_BL_TMI: Total magnetic intensity (TMI) colour image and contours.

JN_20k_BL_TauSF: dB/dt Calculated Time Constant (Tau) with contours of anomaly areas of the Calculated Vertical Derivative of TMI
JN_20k_BL_TotHGrad: Magnetic Total Horizontal Gradient colour image.
JN_20k_BL_TiltDrv: Magnetic Tilt-Angle Derivative colour image.

JN represents job number (AQ130191)
BL represents block name (Dinty)

Maps are also presented in PDF format.

- 1:50,000 topographic vectors were taken from the NRCAN Geogratis database at; <http://geogratis.gc.ca/geogratis/en/index.html>.
- A Google Earth file *AQ130191_FP.kml* showing the flight path of the block is included. Free versions of Google Earth software from: <http://earth.google.com/download-earth.html>

6. INTERPRETATION SUMMARY

Upon requests of Canexplor Management, the following additional products were prepared by Aeroquest Airborne for the Dinty Lake property flown with VTEM-Mag system:

- Calculated time-constant (Tau) analysis from dBz/dt data;
- Resistivity-depth-Images (RDI) of 3 lines;
- Identification of anomalous zones.

6.1 Geological Setting

Dinty Lake property is located in the metamorphosed terrains of the Precambrian shield of northern Saskatchewan, between longitude 107.52° to 107.57° west and latitude 59.36° to 59.39° north.

The property is hosted by gneiss rocks (Rgf) from the Beaverlodge domain, Rae province, as indicated by the Bedrock Geology of Saskatchewan².

6.2 Tau Parameters and CVG Calculation

The processed VTEM survey results are presented as calculated dBz/dt time constant (Tau), which is an indicator of geological unit's electrical conductance.

An explanation of the EM time constant (Tau) calculation is provided in Appendix E. The Tau dBz/dt map is presented in Appendix C. The map is accompanied by an overlay of the calculated vertical gradient (CVG) of TMI anomaly contours for tracking possible EM-Mag anomaly correlation.

The CVG contour layer on top of Tau color grid is more representative of the smaller scale and shallower magnetic sources in comparison with TMI map. It is designed to emphasize the structures and lithological units that might not otherwise be seen on the TMI map due to the nearby presence of stronger magnetic responses, showing much better resolution in terms of individual structures, than the TMI map.

The time-constant (Tau) image with CVG contours is presented in Figure 7. Flight path of the VTEM survey over Dinty Lake property is also presented.

² Saskatchewan Ministry of Energy and Resources, 2013. Bedrock geology layer merged from 1:250,000 scale Compilation Bedrock Geology map series; Geological Atlas of Saskatchewan downloaded from website http://www.infomaps.gov.sk.ca/website/SIR_Geological_Atlas/viewer.htm

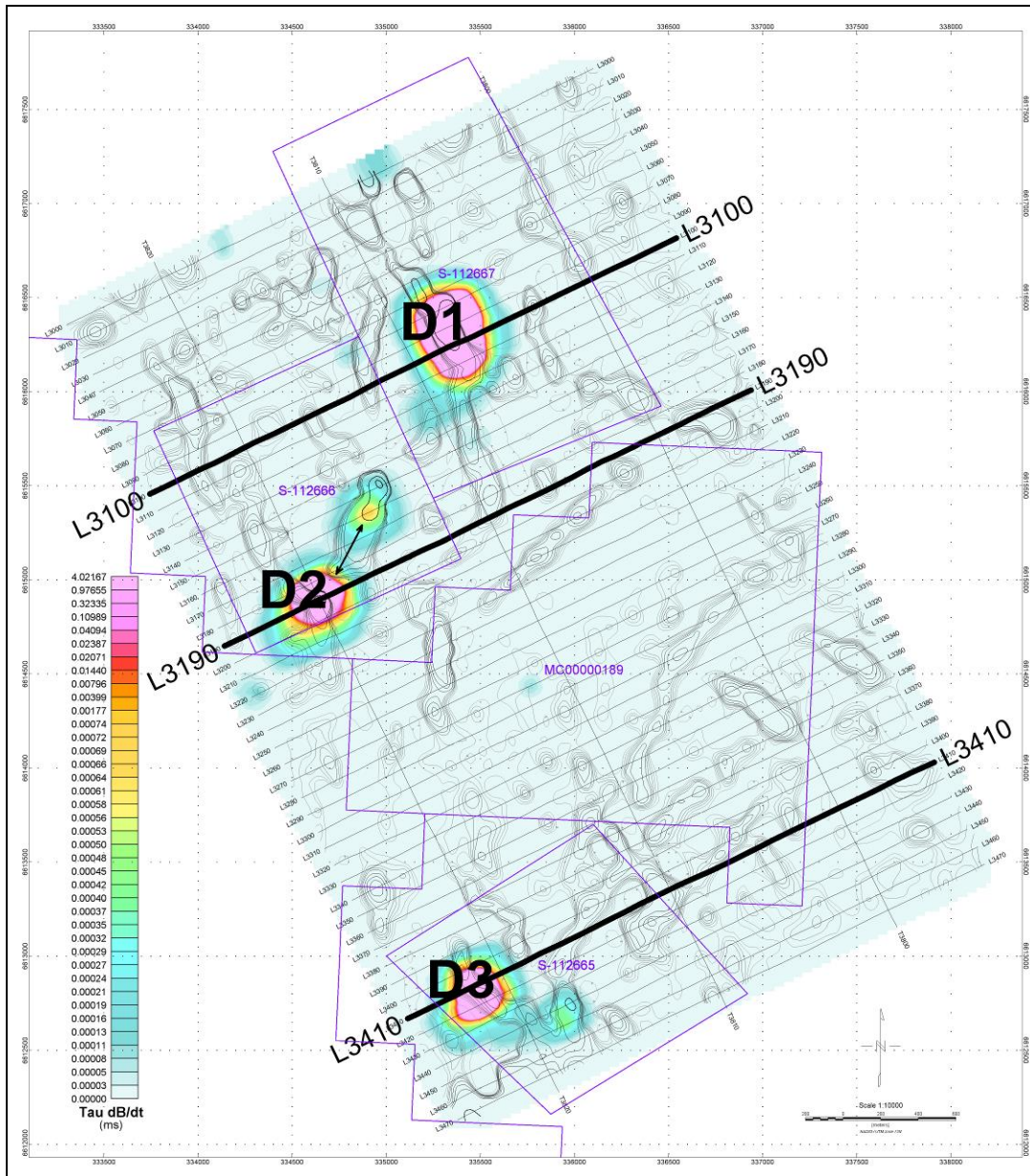


Figure 7 – Image of Time Constant (Tau, dB/dt) and Calculated Vertical Gradient (CVG) of TMI contours, highlighting flight path of RDIs – Dinty Lake property

TEM anomalies are considered to be induced by moderate local conductive targets, exhibiting a time-constant (Tau) up to 4.2ms. TEM response is visible in all time gates range (in dB/dt and B-field data), consistent in the X-coil and Z-coil data. Magnetic association is observed with TEM anomalies.

6.3 Resistivity Depth Imaging

The basis of the Resistivity-Depth Image (RDI) method for TEM data presentation is described in Appendix F. Results of the RDI one-dimensional (1D) fast transformation provide a first geometric approximation of the conductor, depth of conductive targets and also the depth of investigation which depends on conductance of the rocks.

Three lines that extend over conductive zones were subjected to the RDI procedure (Figure 7). Cross sections accompany this report in digital raster format and in Geosoft format. RDIs are presented in subsequent sections according to selected anomalies.

A 3D voxel of RDI constructed from all survey lines is shown in Appendix C of this report.

6.4 Identification of Anomalous Zones

Several anomalous zones (D1, D2, D3) are identified in the property.

Zone D1

It is located 300 m east of the long north-northwest trending bay of Dinty Lake.

The anomaly is observed on 500 m along strike in a wide conductive trend between survey lines L3070 to L3120. The RDI of L3100 shows a wide conductor as the main zone; with a slightly thin sub-vertical conductor (double-pick anomaly) indicating a target dipping to the west. Apparent resistivity < 6 ohm-m is observed at this location (Figure 8 below); with highest time-constant (Tau) of 4.2 milliseconds. Magnetic correlation is observed.

There is a known Ni deposit register in the mineral deposit index of the province of Saskatchewan (SMDI 1603³) coinciding with anomalous zone D1.

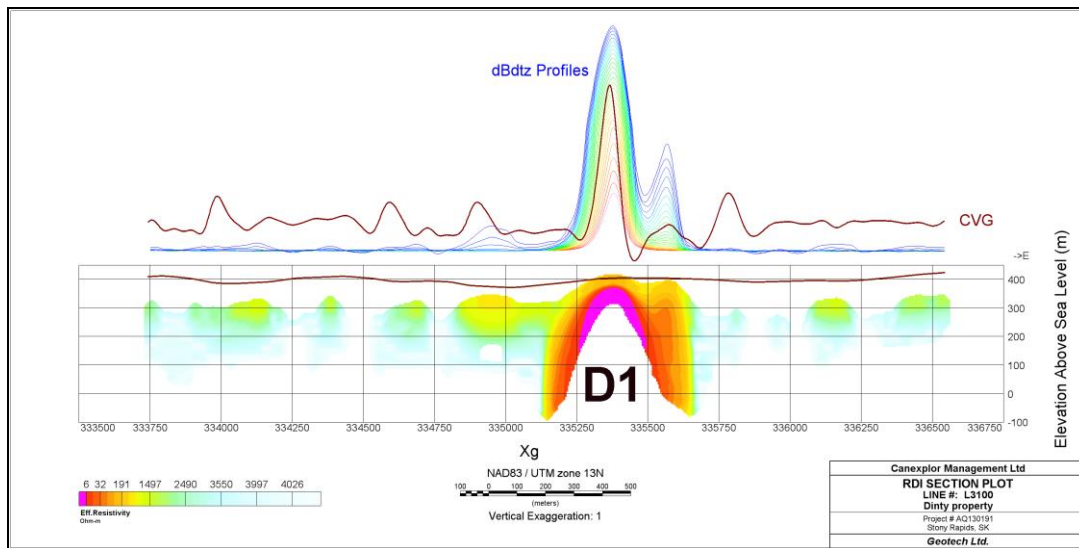


Figure 8 – Resistivity Depth Image (RDI) of L3100, anomaly D1 – Dinty Lake property

The geology of this Ni deposit, according to SDMI 1603, indicates that the area is underlain by a small sill-like norite body. The norite is enclosed in felsic gneisses of the Nivens domain. The rocks have been metamorphosed to granulite facies. The norite has been dated at 2.55 ± 0.23 Ma using Nd-Sm methods. The norite intrusive is a layered body of anorthosite, anorthositic norite, norite, feldspathic pyroxenite, pyroxenite and their metamorphic equivalents.

³ Online reference <http://www.er.gov.sk.ca/dbsearch/MinDepositQuery/default.aspx?ID=1603>

The main mineralized norite body has a northerly trend and dips to the west; confirmed by the VTEM results. At a depth of 200 ft (61 m) the body apparently narrows and ends. The ore zone is at least 300 m (984.3 ft) long and 65 m (213.3 ft) wide.

The mineralization consists of pyrrhotite as cementing material, fracture fillings and disseminations. Small amounts of chalcopyrite and sphalerite are present. Molybdenite has been reported. Cubanite occurs as spherical inclusions in the pyroxenes. The greatest accumulation of sulphides is underlain by a thin layer of orthopyroxenite that is, in turn, underlain by norite.

Drilling, completed between 1936 and 1942, outlined a deposit. Selected samples assayed up to 0.94% Ni, 0.04% Cu, 0.01 oz./ton Au and 0.10 oz./ton Ag. The main body has a maximum width of 200 ft (61.0 m) and has been traced by 8 trenches and outcrops for 900 ft (274.3 m).

Zone D2

It is located southwest of Dinty Lake, representing a circular-shape conductive zone observed between survey lines L3180 to 3200 and tie-line T3820.

In this anomalous zone, highest values of Tau (3.5 ms) are observed in L3190. Its RDI exhibits apparent resistivity < 6 ohm-m with a near surface conductive response. Magnetic correlation is observed.

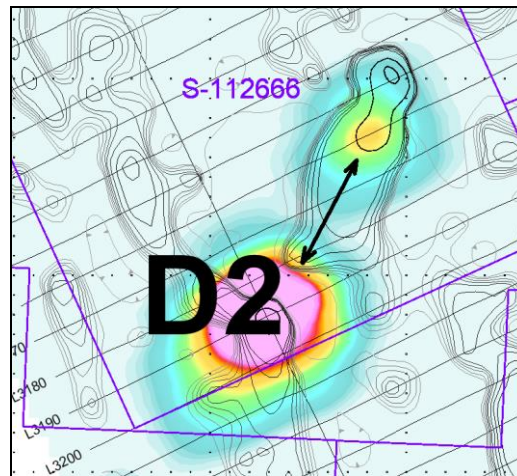


Figure 9 – Tau image and CVG contours of TMI, highlighting conductive anomalies and magnetic lineaments (black arrow) that cross-cut where anomalous zone D2 is identified – Dinty Lake property

In order to identify electrical properties of individual targets, further calculation of RDIs and Maxwell plate modeling is recommended at this location.

Zone D3

Located in the south part of the survey block, this anomalous zone is detected between lines L3400 to L3420.

The anomaly exhibits complex geometry as seen in dB/dt and Bfield data in the Z-coil and X-coil measurements. Highest Tau values are observed on line L3410, up to 4.2 ms. RDI of L3410 shows apparent resistivity < 9 ohm-m at about 50m depth (Figure XX). This conductive response is associated to magnetic anomalies.

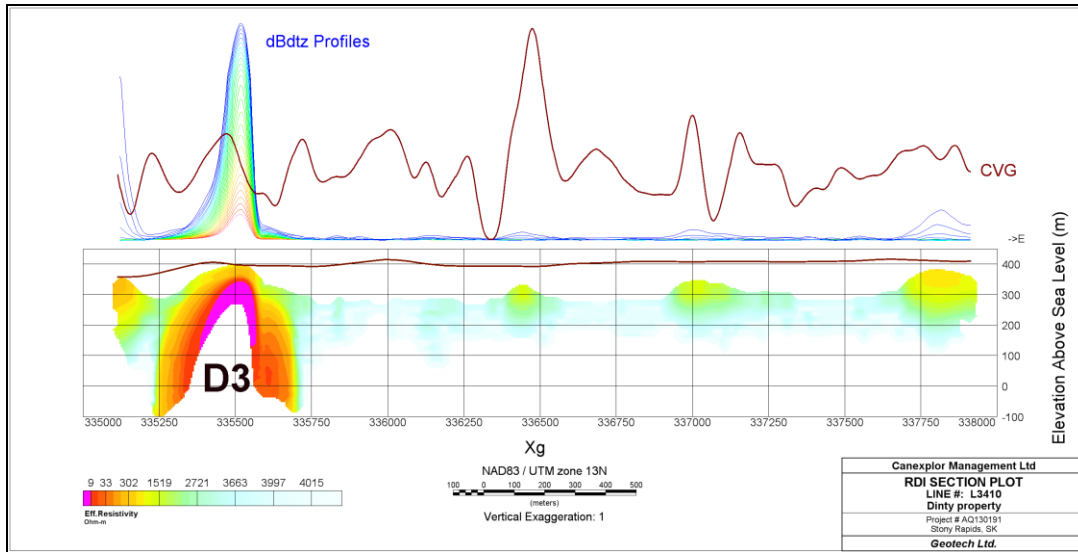


Figure 10 – Resistivity Depth Image (RDI) of L3410, anomalous Zone D3 – Dinty Lake Property

Selected anomalous zones (D1, D2, D3) are presented in Figure 11. Profiles of dBz/dt response overlaying the magnetic Tilt derivative of Dinty Lake property are shown, highlighting identified anomalous zones.

The magnetic Tilt derivative is calculated from the measured horizontal gradients and the calculated vertical gradient. It represents a useful tool for identifying target edges. As observed in figure below, all conductive anomalous zones are located adjacent to a fault system (black dash lines); representing a favourable control for potential mineralization in Dinty Lake property.

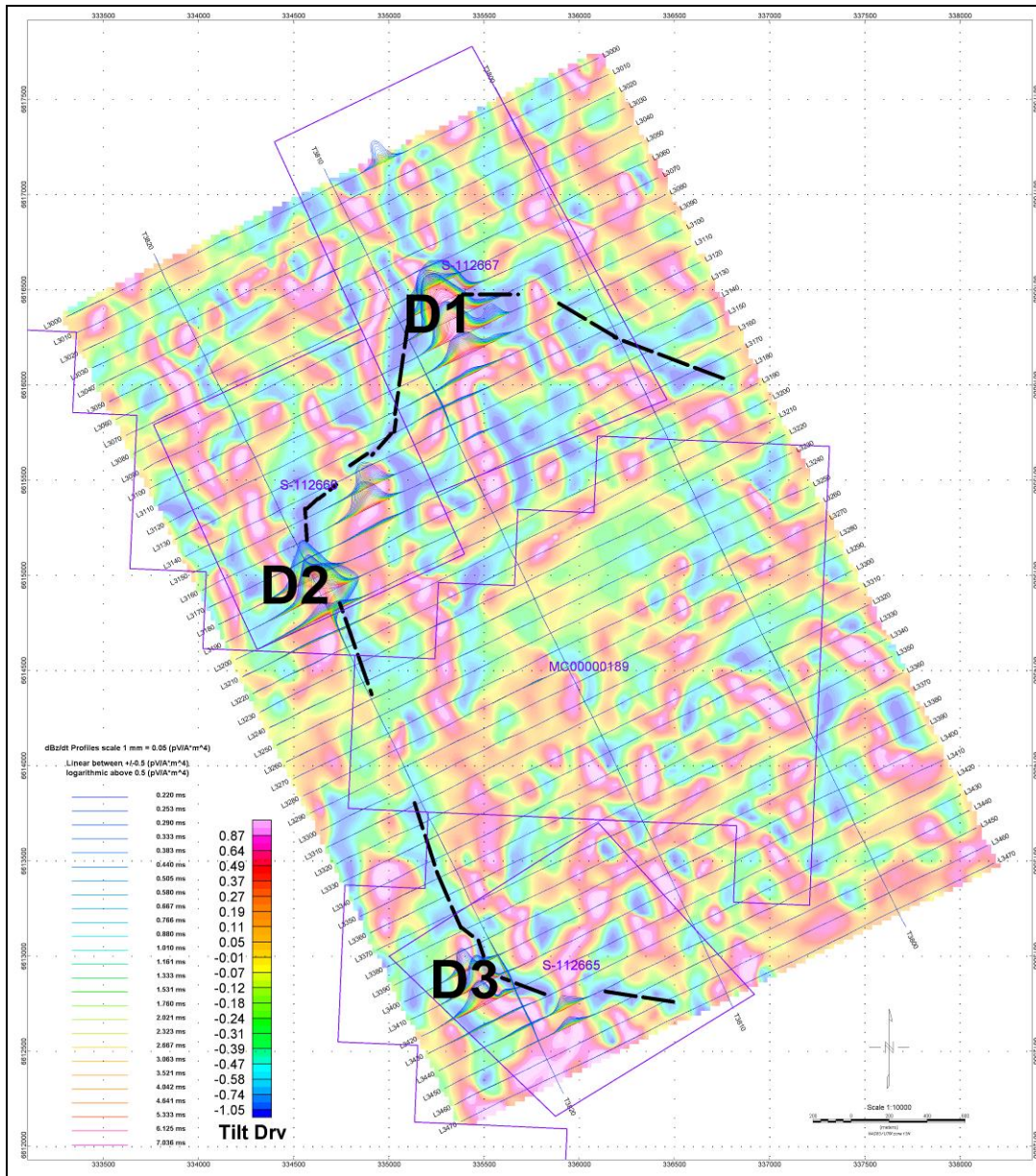


Figure 11 – VTEM profiles of dBz/dt overlaying the magnetic Tilt derivative (rendering transparency) and recommended anomalous zones (D1, D2, D3) to follow-up – Dinty Lake property

7. CONCLUSIONS AND RECOMMENDATIONS

A helicopter-borne versatile time domain electromagnetic (VTEM) geophysical survey has been completed over the Dinty Lake property area near Stony Rapids, Saskatchewan, Canada.

The total area coverage is 15 km². Total survey line coverage is 158 line kilometres. The principal sensors included a Time Domain EM system and horizontal magnetic gradiometer using two cesium magnetometers. Results have been presented as stacked profiles, and contour colour images at a scale of 1:10,000. A formal Interpretation has not been included .

Based on the geophysical results obtained, roughly three major TEM anomalous zones are identified across the property. The conductive anomalous zones are indicated on the map below.

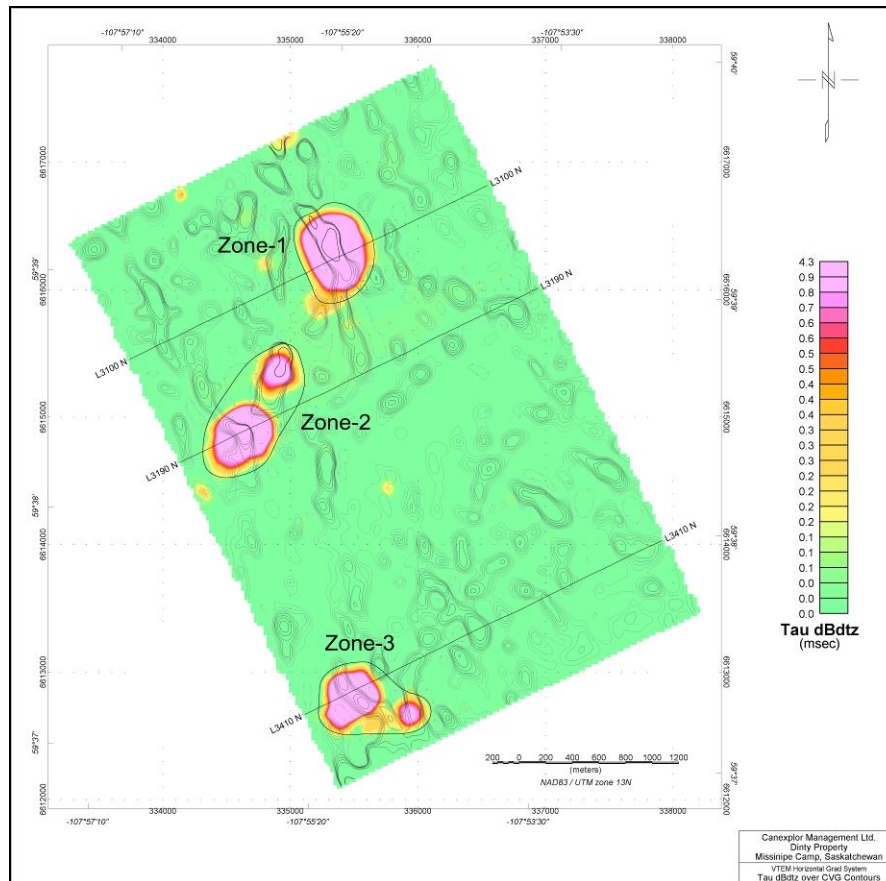


Figure 12 – Tau dB/dt Z over CVG contours showing the anomalous zones

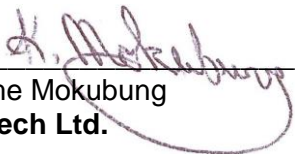
Zone 1 is a discrete conductor oriented NW-SE. The EM response of the conductor is about 800m long. The zone is closely associated with a magnetic anomaly. According to detail resistivity depth imaging, the top of the EM anomaly source is around on 80-100m depth (reference on L3100 RDI).

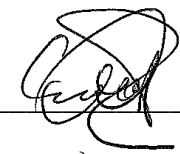
Zone 2 consists of two discrete shallow conductors trending NE-SW and is associated with two separate magnetic anomalies (reference on L3190 RDI).

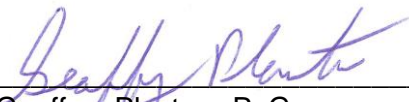
Zone 3 consists of two discrete dipping conductors. The conductors are separated by a potential NE-SW fault. According to detail resistivity depth imaging, the top of the target is approximately 25-50 m depth (reference on L3410 RDI).

If the conductors correspond to an exploration model on the area it is recommended picking anomalies with conductance grading and center localization of the targets, detail resistivity depth imaging and plate Maxwell modelling with test drillhole parameters prior to ground follow up and drill testing.

Respectfully submitted⁴,


Keeme Mokubung
Geotech Ltd.

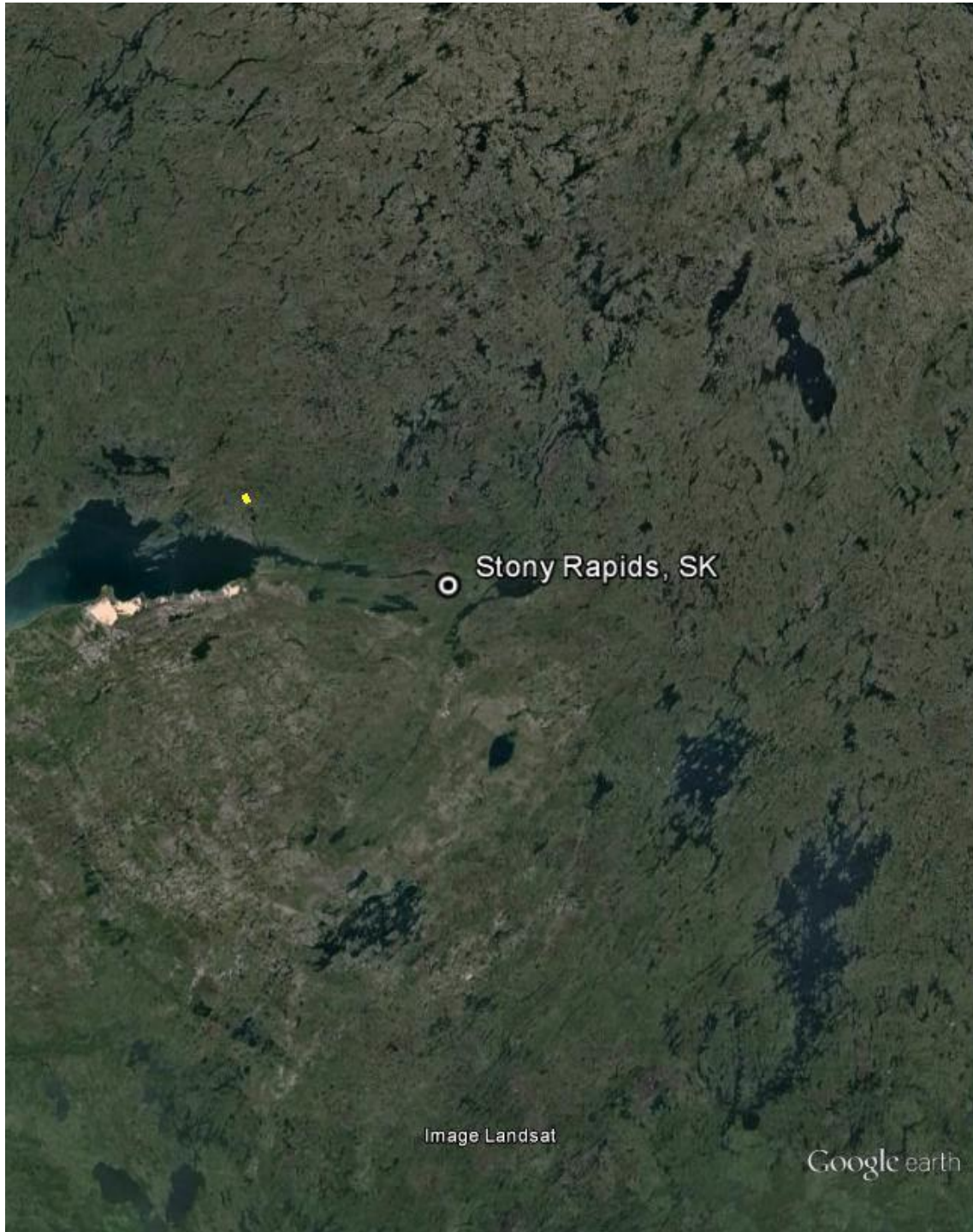

Marta Orta
Geotech Ltd.


Geoffrey Plastow, P. Geo.
Data Processing Manager
Geotech Ltd.

June 2013

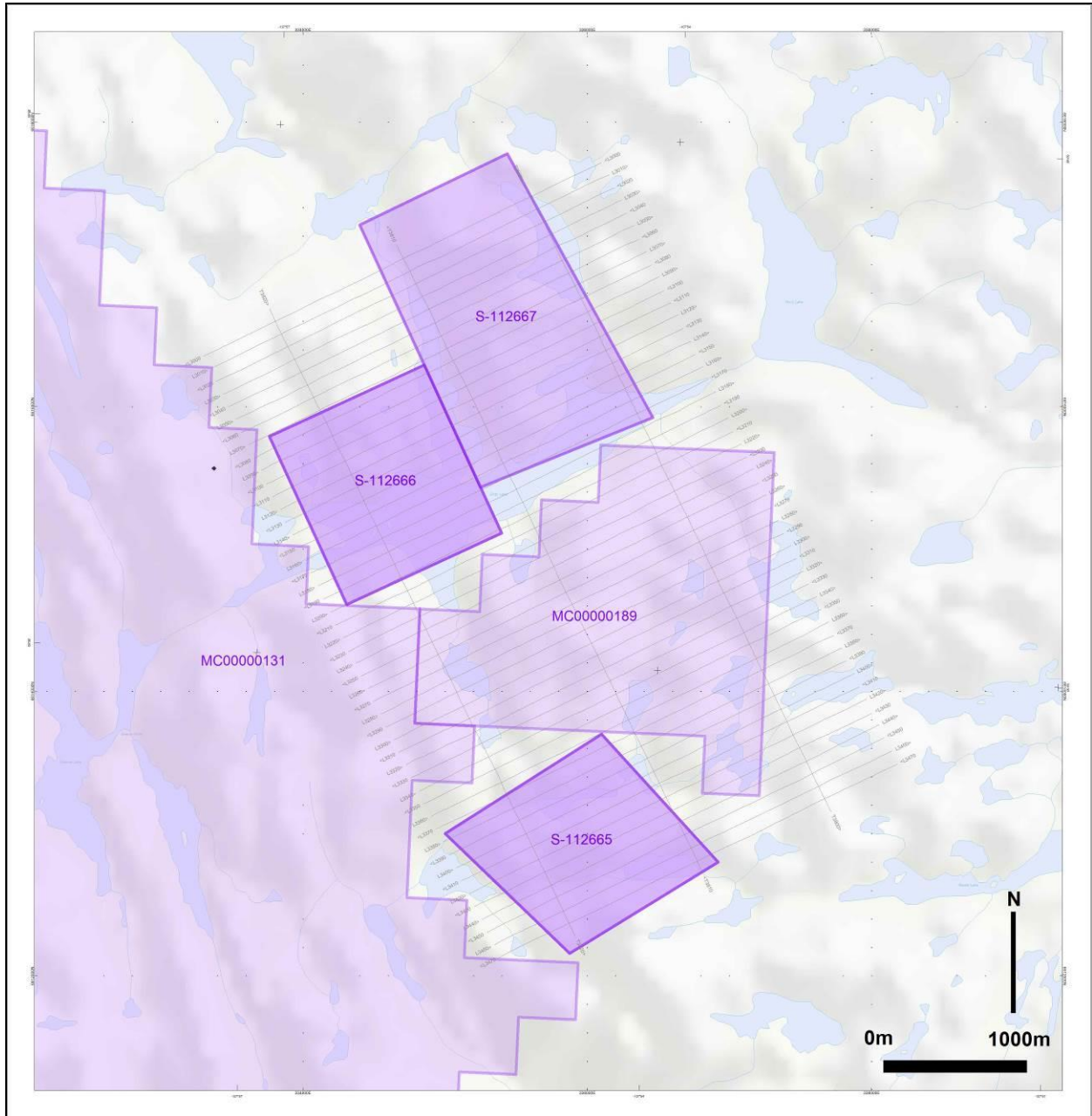
⁴ Final data processing of the EM and magnetic data were carried out by Keeme Mokubung, from the office of Geotech Ltd. in Aurora, Ontario, under the supervision of Geoffrey Plastow, P. Geo., Data Processing Manager.

APPENDIX A
SURVEY BLOCK LOCATION MAP



Survey Overview of the Survey Area

MINING CLAIMS MAP – DINTY LAKE PROPERTY

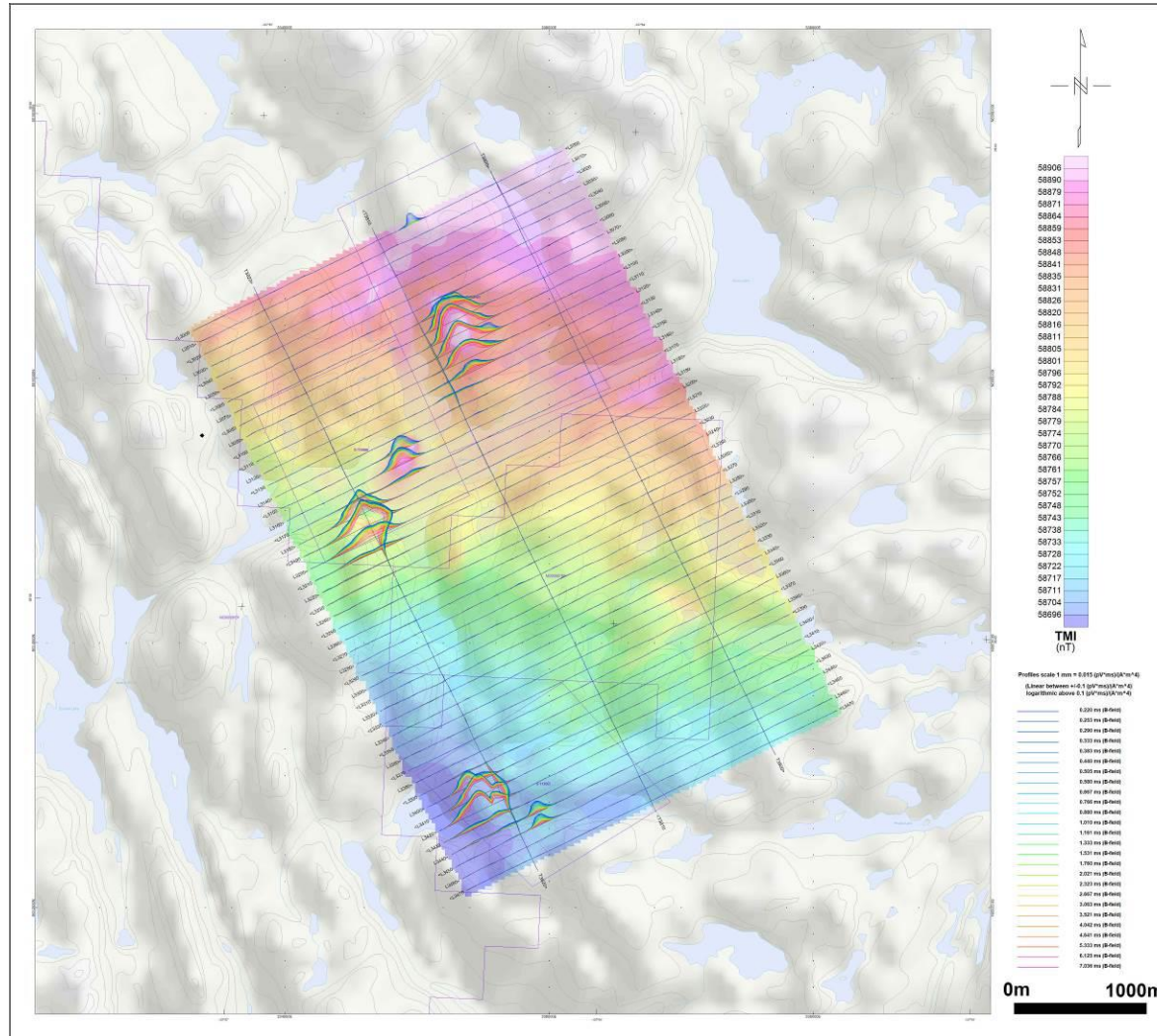


APPENDIX B

DINTY LAKE PROPERTY SURVEY BLOCK COORDINATES (WGS 84, UTM Zone 13 North)

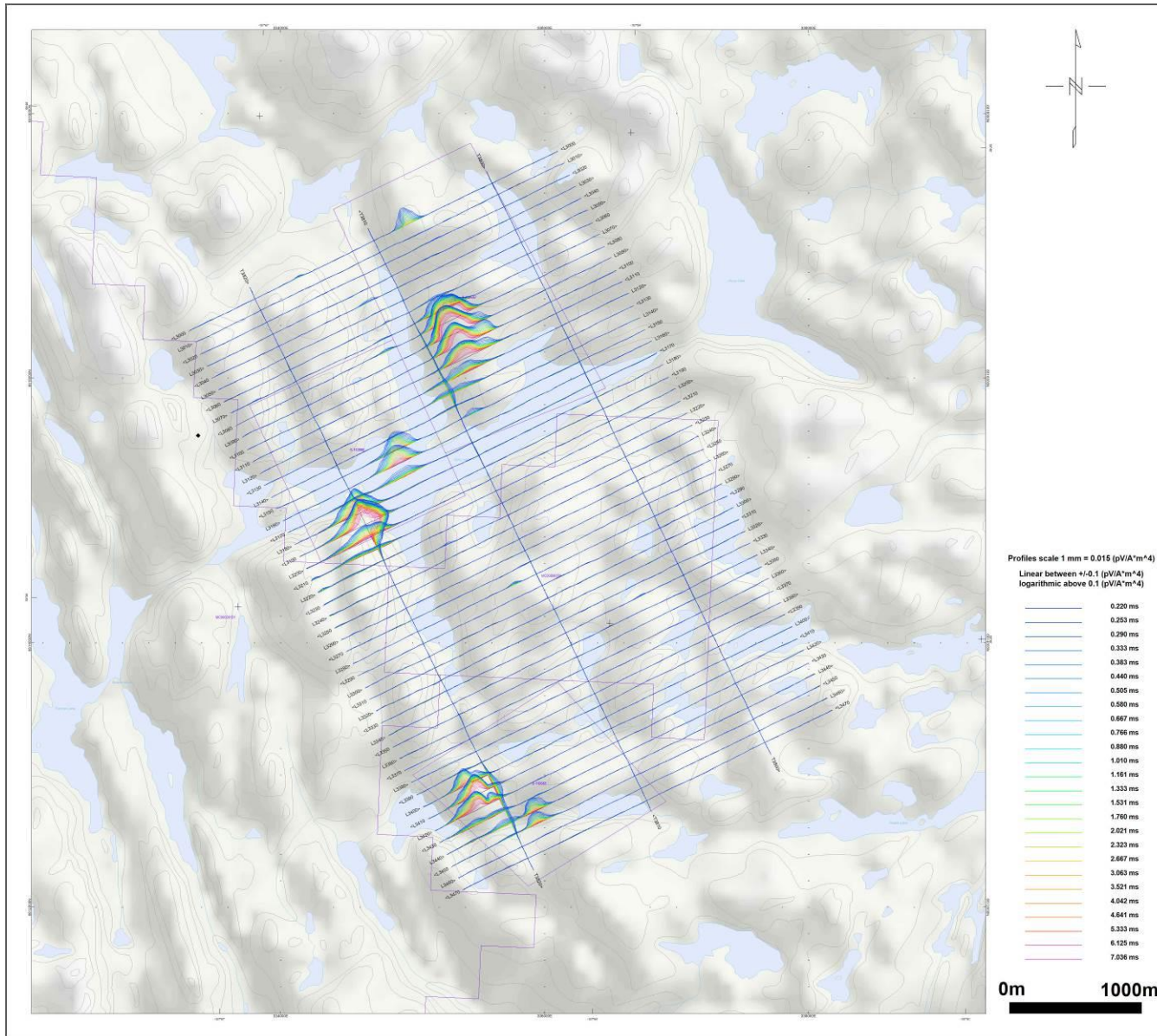
X	Y
333355.1	6616380.5
335435.7	6612150.2
338135.8	6613464.7
336055.3	6617694.9

APPENDIX C GEOPHYSICAL MAPS¹

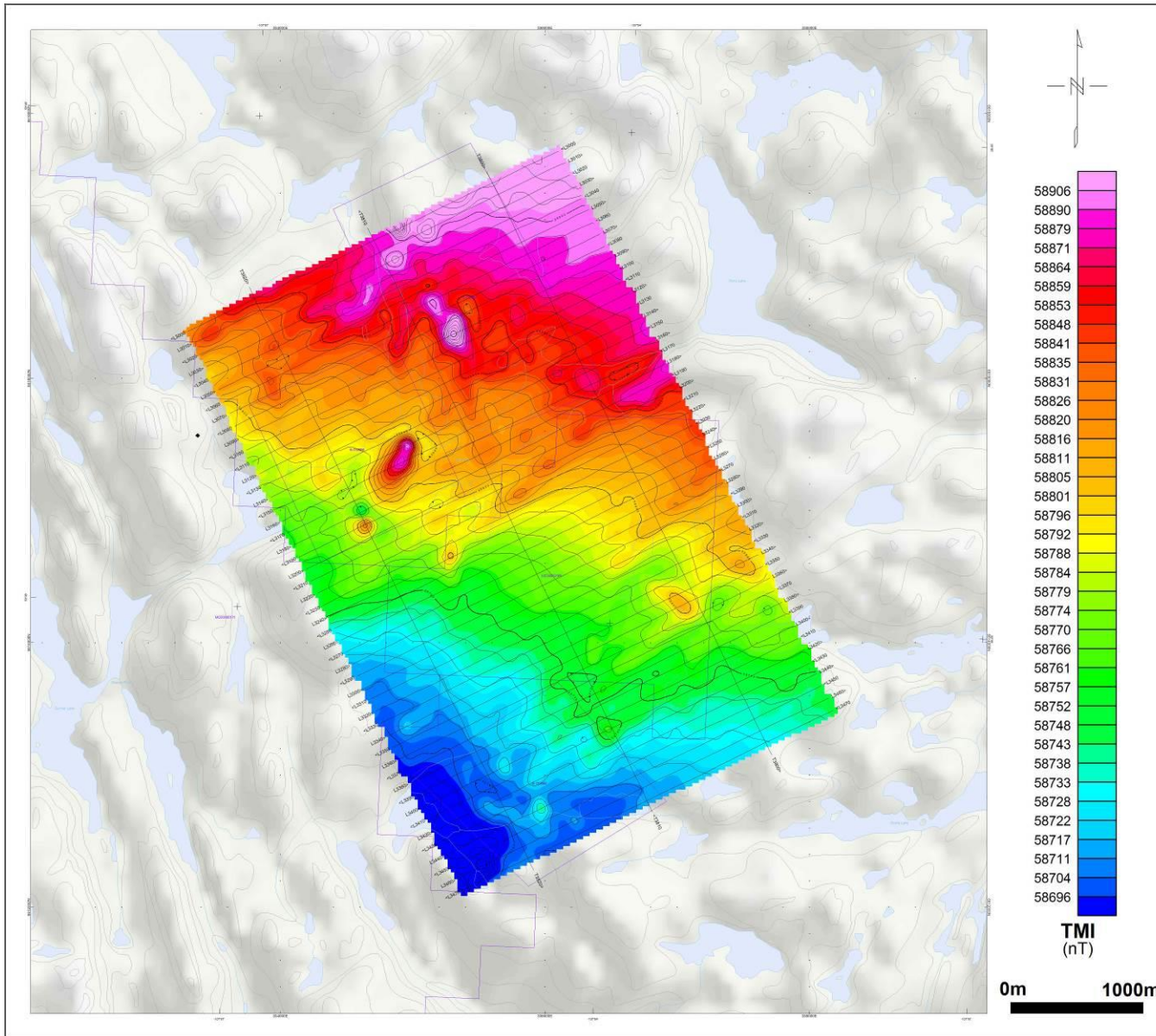


Dinty Lake – VTEM B-Field Z Component Profiles – Time Gates 0.220 – 7.036 ms – Over Total Magnetic Intensity Grid

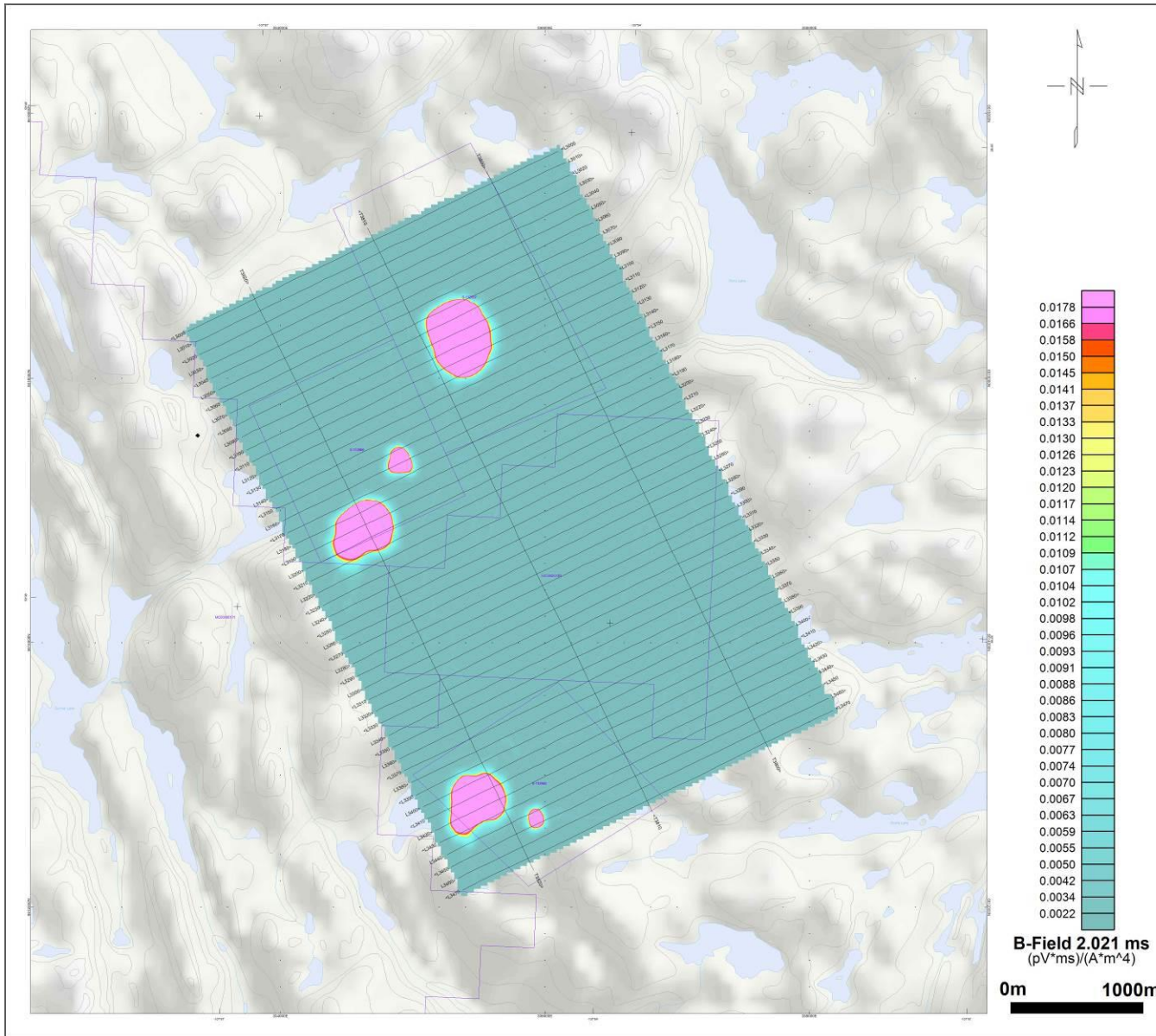
¹ Full size geophysical maps are also available in PDF format on the final DVD



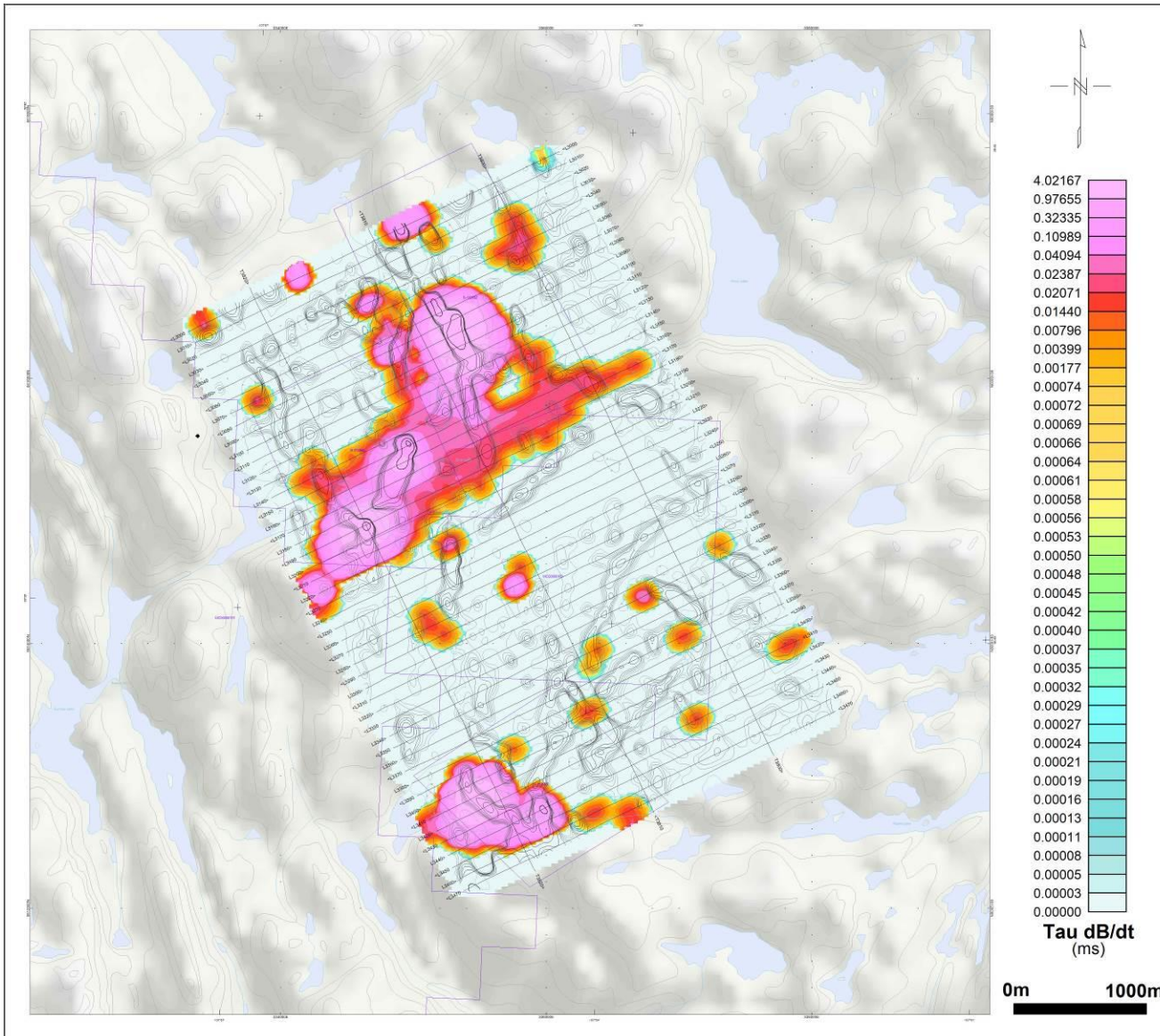
Dinty Lake – VTEM dB/dt Z Component Profiles – Time Gates 0.220 – 7.036 ms



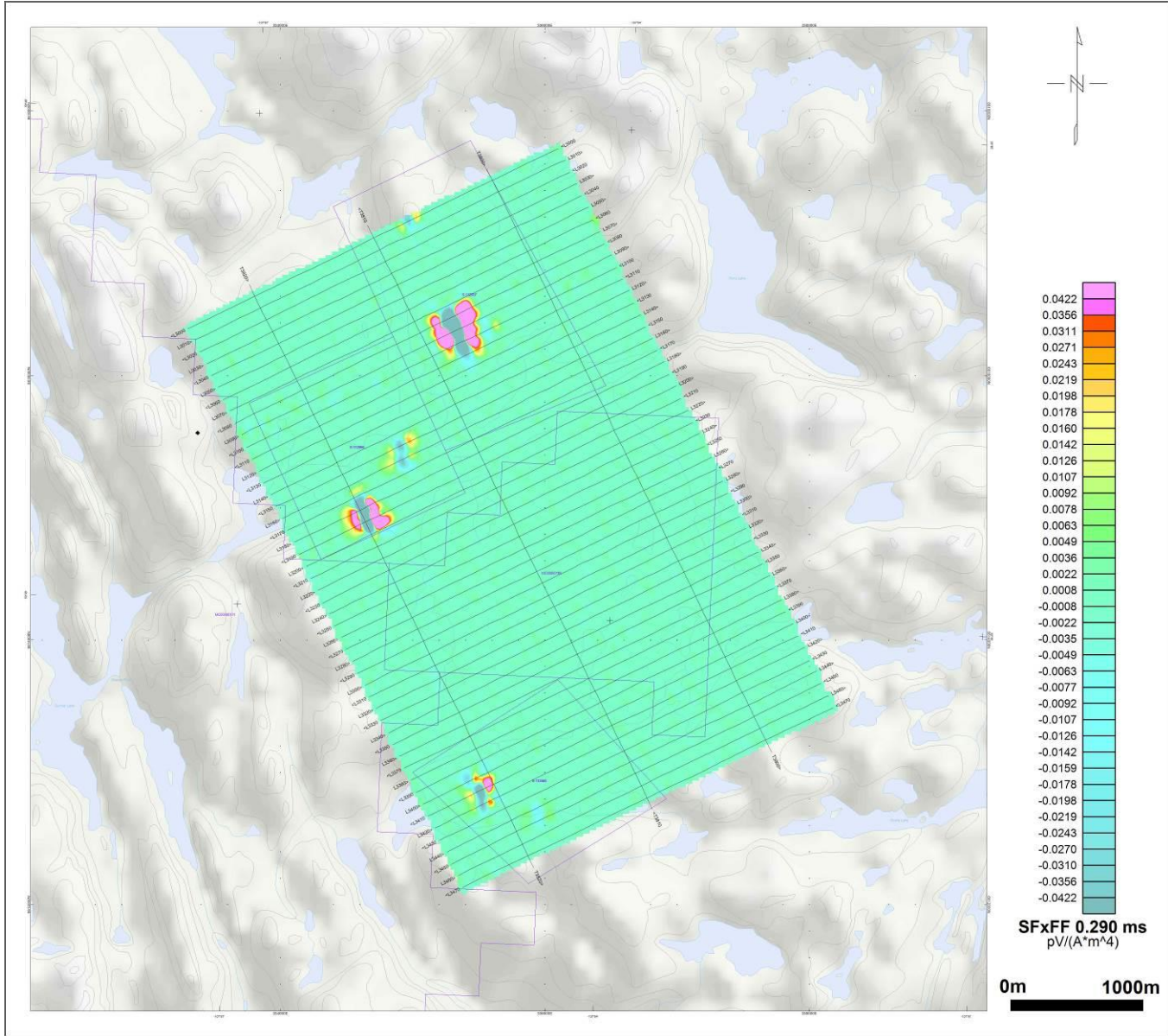
Dinty Lake – Total Magnetic Intensity (TMI)



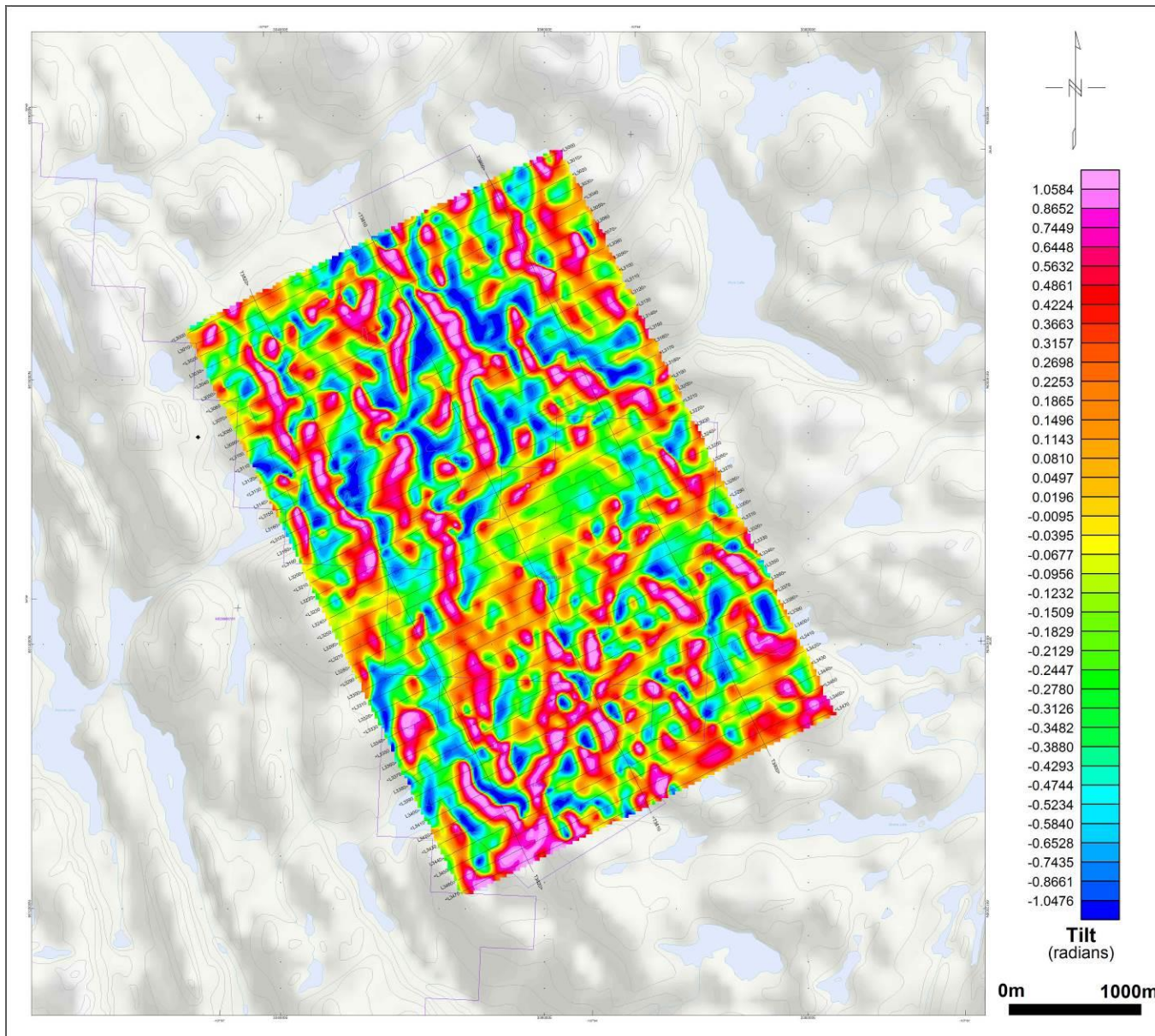
Dinty Lake – VTEM B-Field Z Component – Channel 36 – Time Gate 2.021 ms



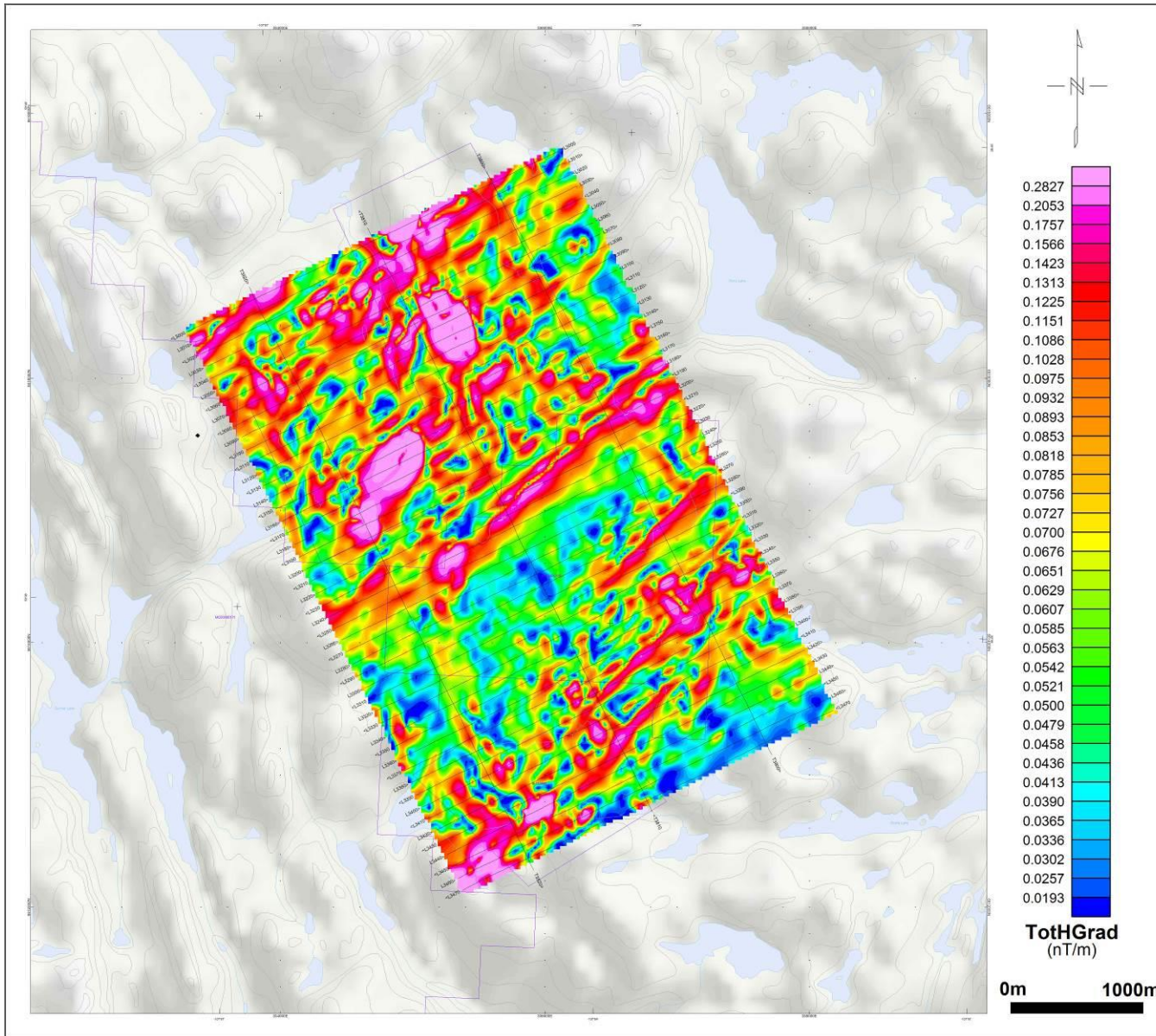
Dinty Lake – dB/dt Calculated Time Constant (Tau) with contours of anomaly areas of the Calculated Vertical Derivative of TMI



Dinty Lake – Fraser Filtered dB/dt X Component – Channel 22 – Time Gate 0.290 ms

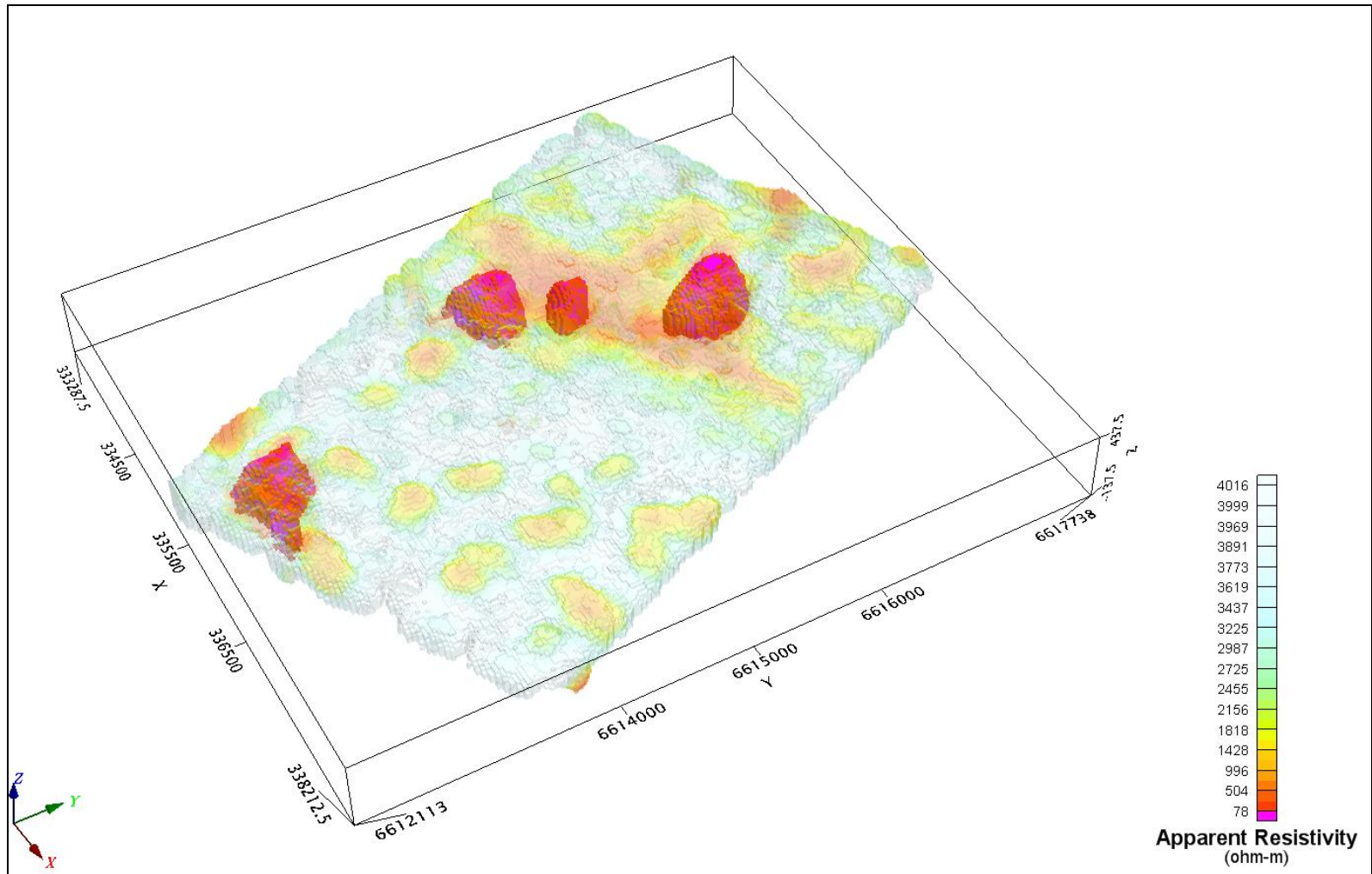


Dinty Lake – Magnetic Tilt-Angle Derivative

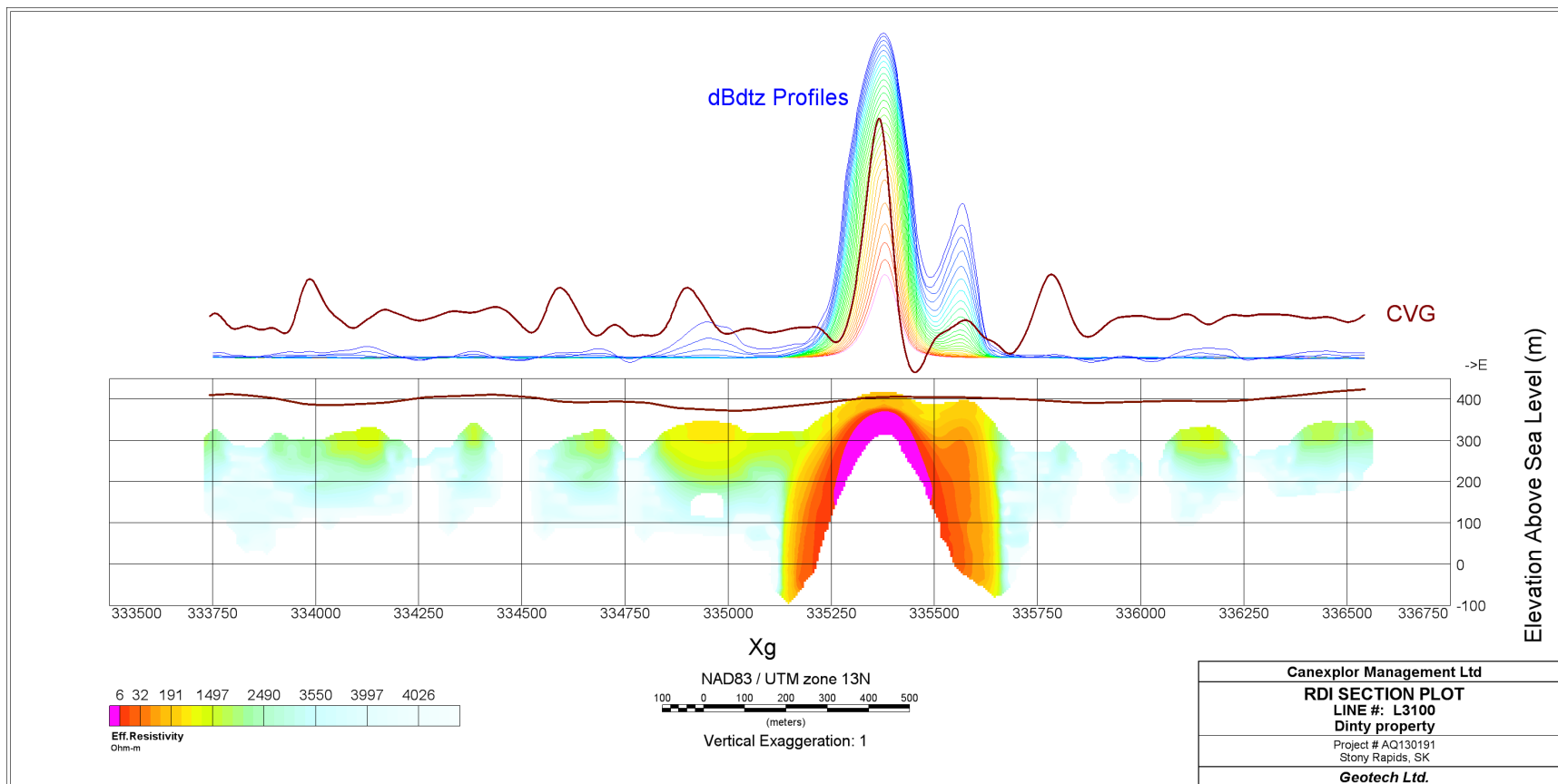


Dinty Lake – Magnetic Total Horizontal Gradient

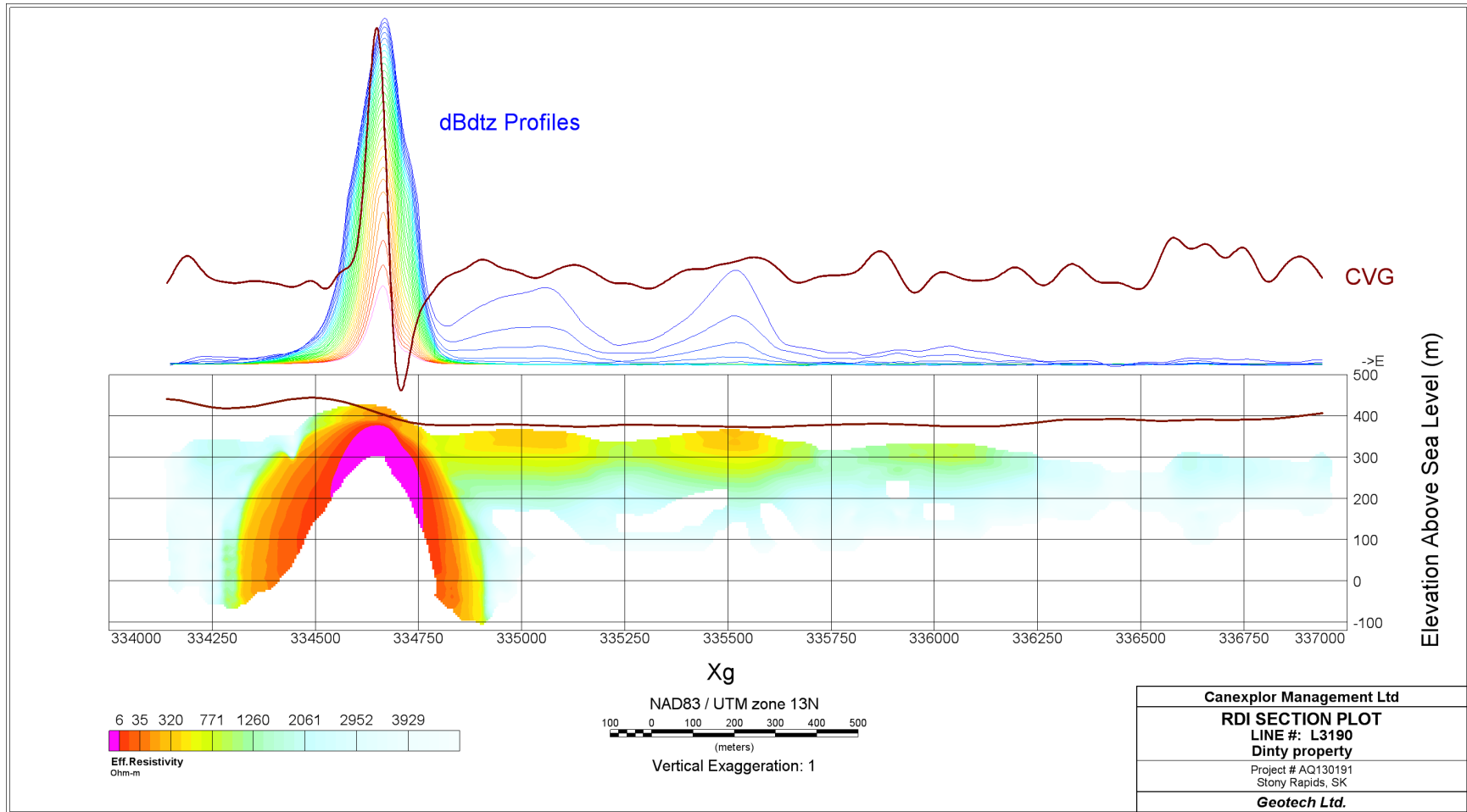
RESISTIVITY DEPTH IMAGE (RDI) MAPS



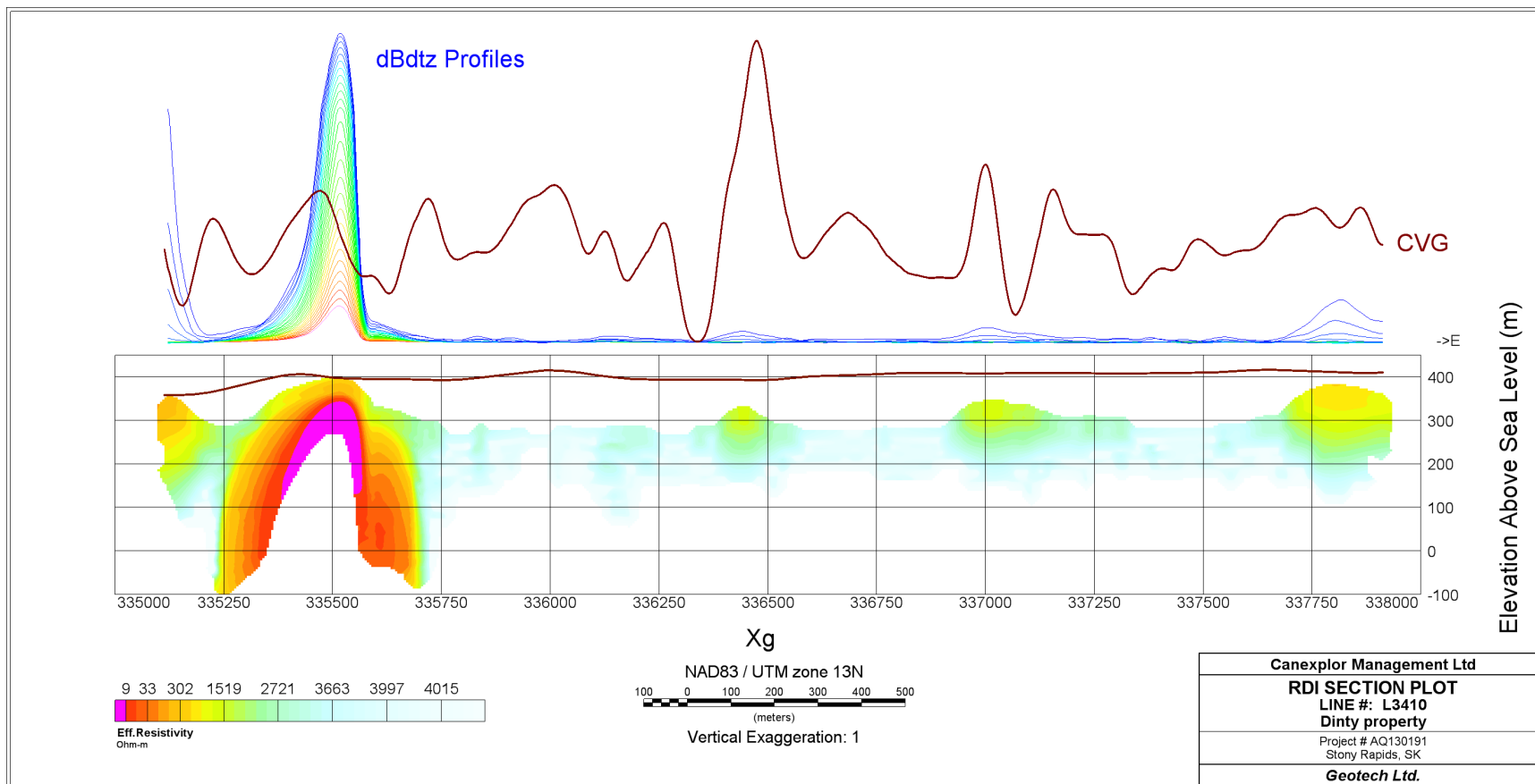
3D Resistivity-Depth Image (RDI)



RDI Section – L3100



RDI Section – L3190



RDI Section – L3410

APPENDIX D

GENERALIZED MODELING RESULTS OF THE VTEM SYSTEM

Introduction

The VTEM system is based on a concentric or central loop design, whereby, the receiver is positioned at the centre of a transmitter loop that produces a primary field. The wave form is a bipolar, modified square wave with a turn-on and turn-off at each end.

During turn-on and turn-off, a time varying field is produced (dB/dt) and an electro-motive force (emf) is created as a finite impulse response. A current ring around the transmitter loop moves outward and downward as time progresses. When conductive rocks and mineralization are encountered, a secondary field is created by mutual induction and measured by the receiver at the centre of the transmitter loop.

Efficient modeling of the results can be carried out on regularly shaped geometries, thus yielding close approximations to the parameters of the measured targets. The following is a description of a series of common models made for the purpose of promoting a general understanding of the measured results.

A set of models has been produced for the Geotech VTEM® system dB/dT Z and X components (see models D1 to D15). The Maxwell™ modeling program (EMIT Technology Pty. Ltd. Midland, WA, AU) used to generate the following responses assumes a resistive half-space. The reader is encouraged to review these models, so as to get a general understanding of the responses as they apply to survey results. While these models do not begin to cover all possibilities, they give a general perspective on the simple and most commonly encountered anomalies.

As the plate dips and departs from the vertical position, the peaks become asymmetrical.

As the dip increases, the aspect ratio (Min/Max) decreases and this aspect ratio can be used as an empirical guide to dip angles from near 90° to about 30°. The method is not sensitive enough where dips are less than about 30°.

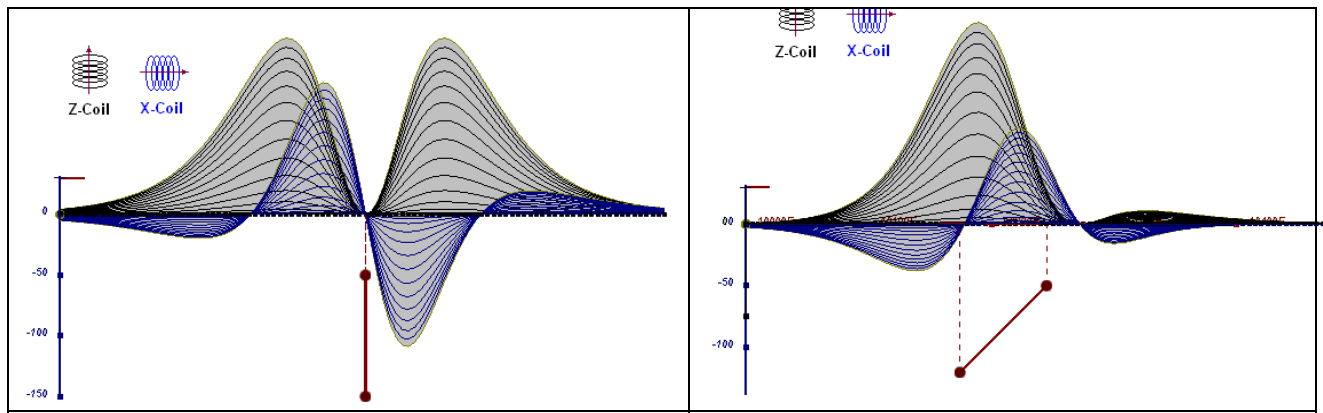


Figure D-1: vertical thin plate

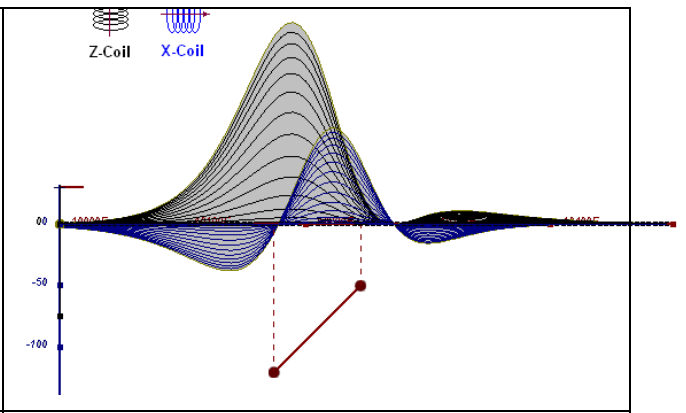


Figure D-2: inclined thin plate

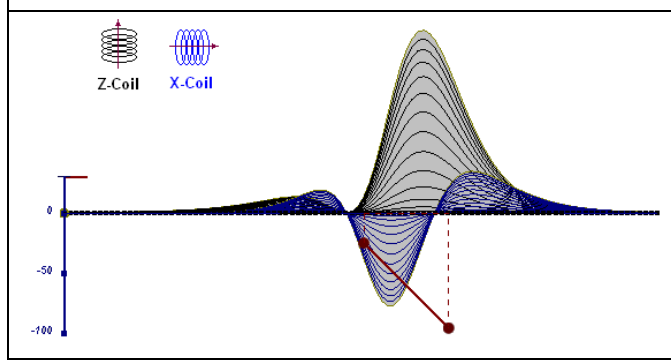


Figure D-3: inclined thin plate

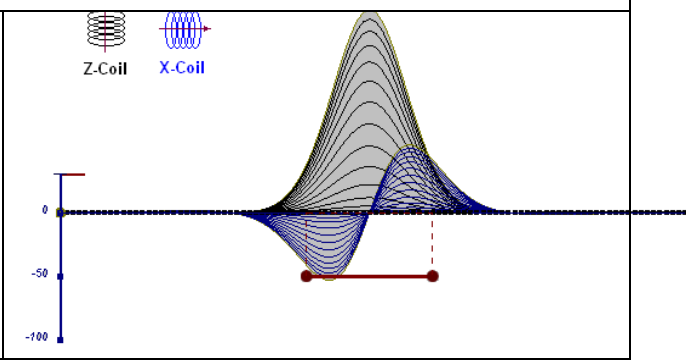


Figure D-4: horizontal thin plate

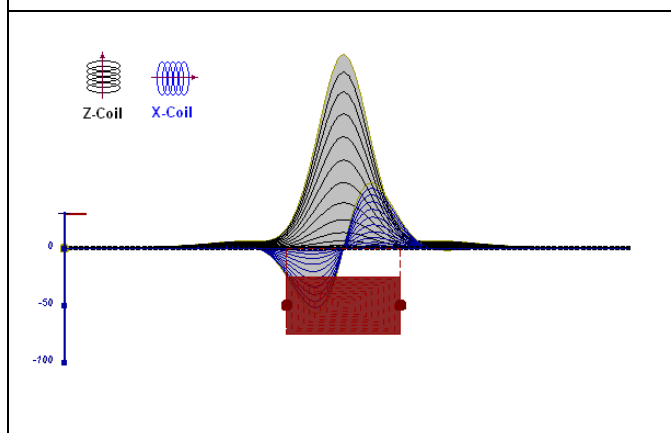


Figure D-5: horizontal thick plate (linear scale of the response)

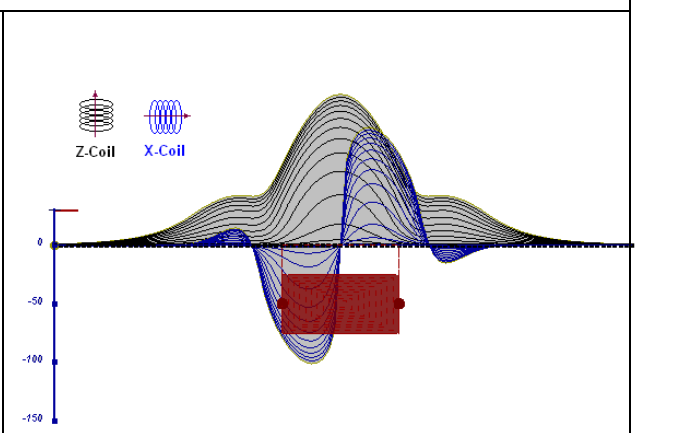


Figure D-6: horizontal thick plate (log scale of the response)

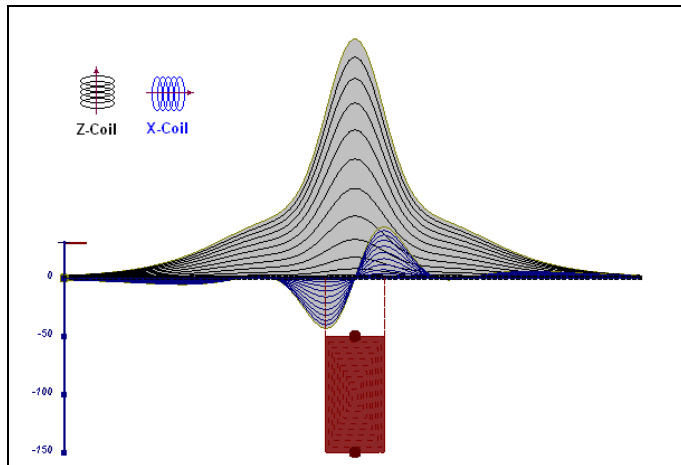


Figure D-7: vertical thick plate (linear scale of the response). 50 m depth

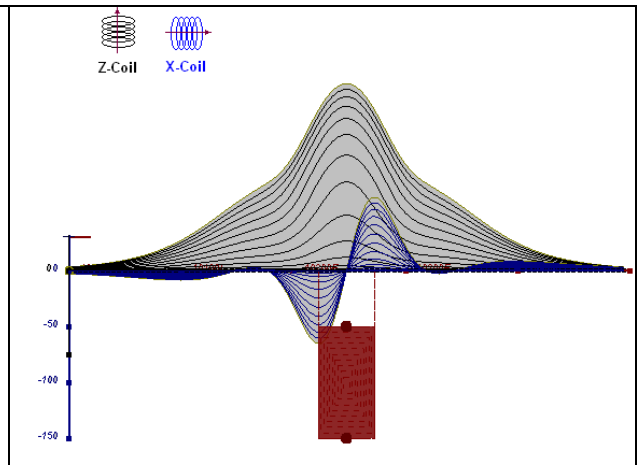


Figure D-8: vertical thick plate (log scale of the response). 50 m depth

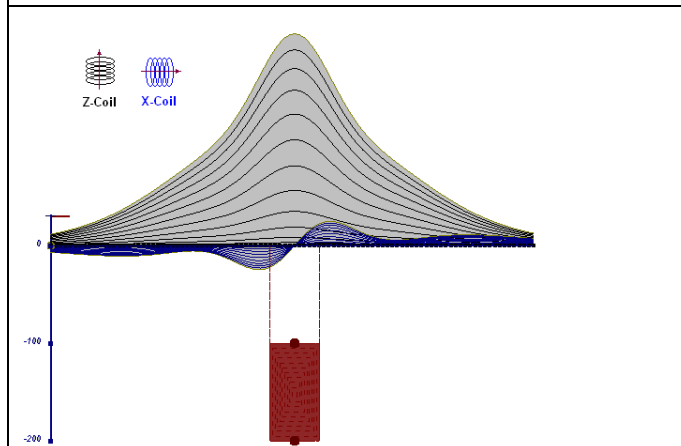


Figure D-9: vertical thick plate (linear scale of the response). 100 m depth

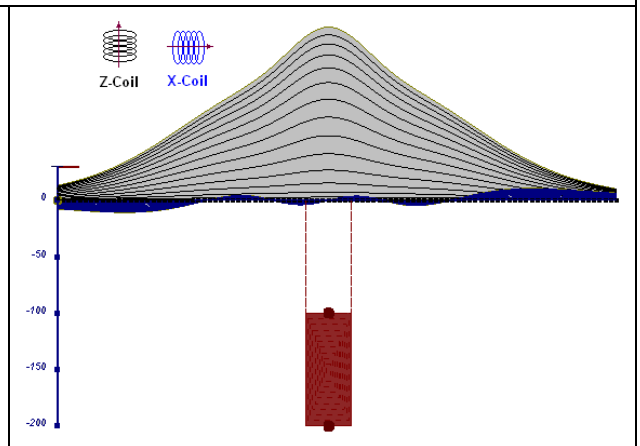


Figure D-10: vertical thick plate (linear scale of the response). Depth/hor.thickness=2.5

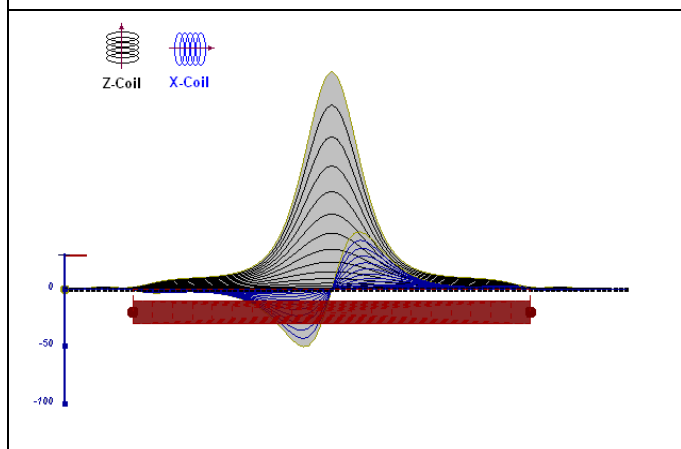


Figure D-10: horizontal thick plate (linear scale of the response)

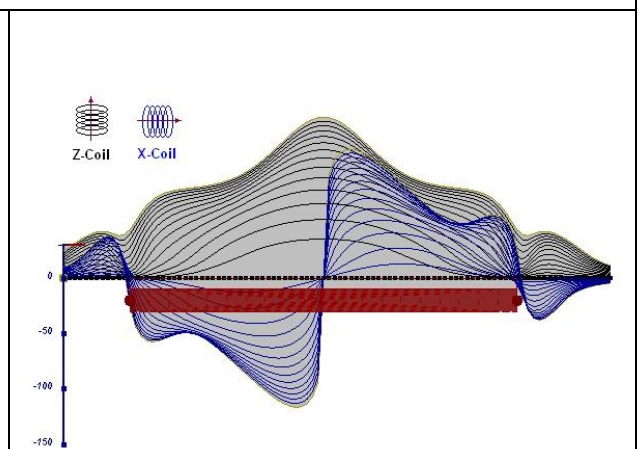


Figure D-11: horizontal thick plate (log scale of the response)

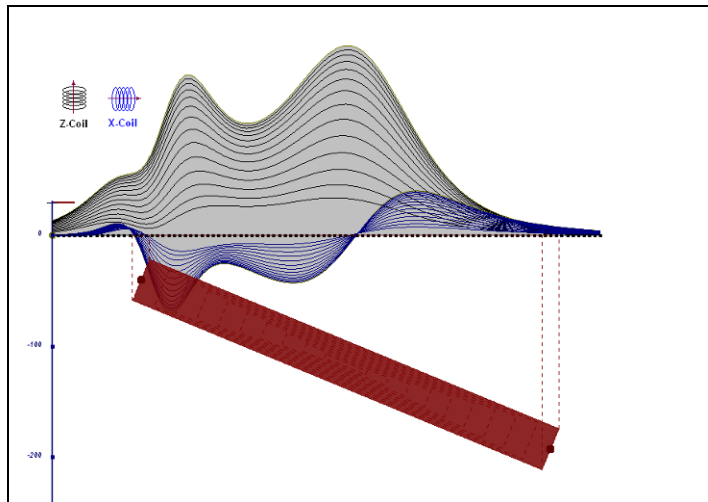


Figure D-12: inclined long thick plate

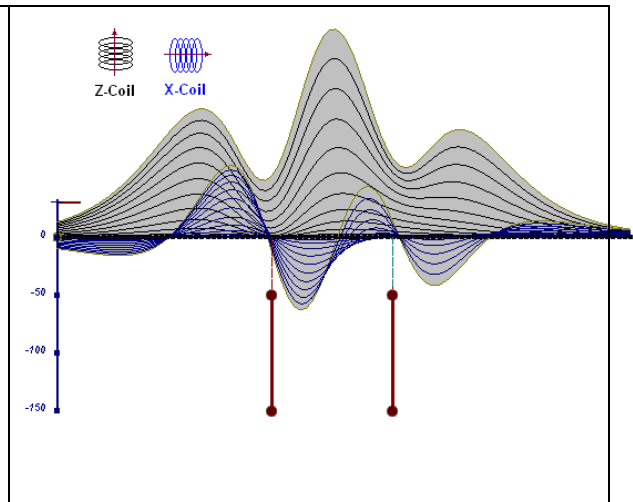


Figure D-13: two vertical thin plates

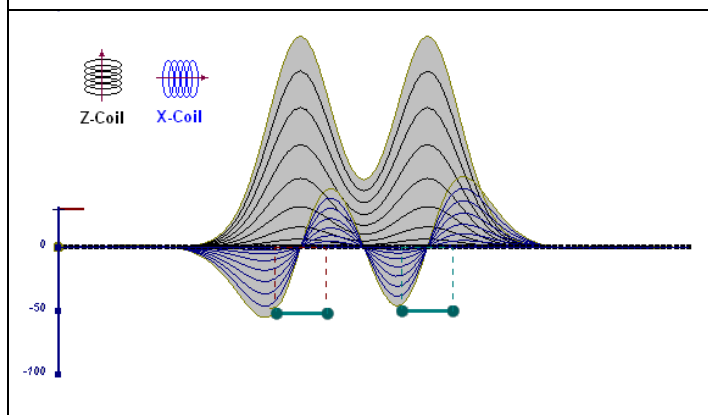


Figure D-14: two horizontal thin plates

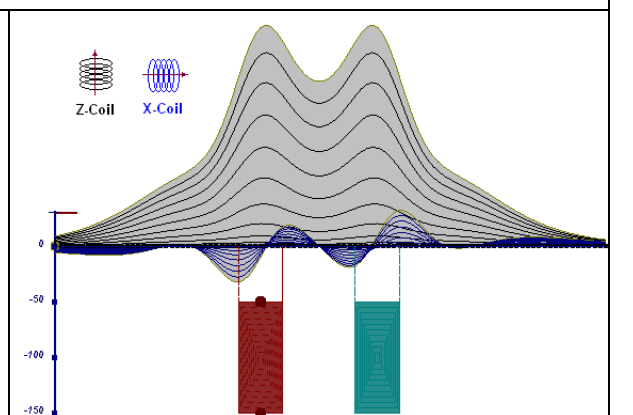


Figure D-15: two vertical thick plates

The same type of target but with different thickness, for example, creates different form of the response:

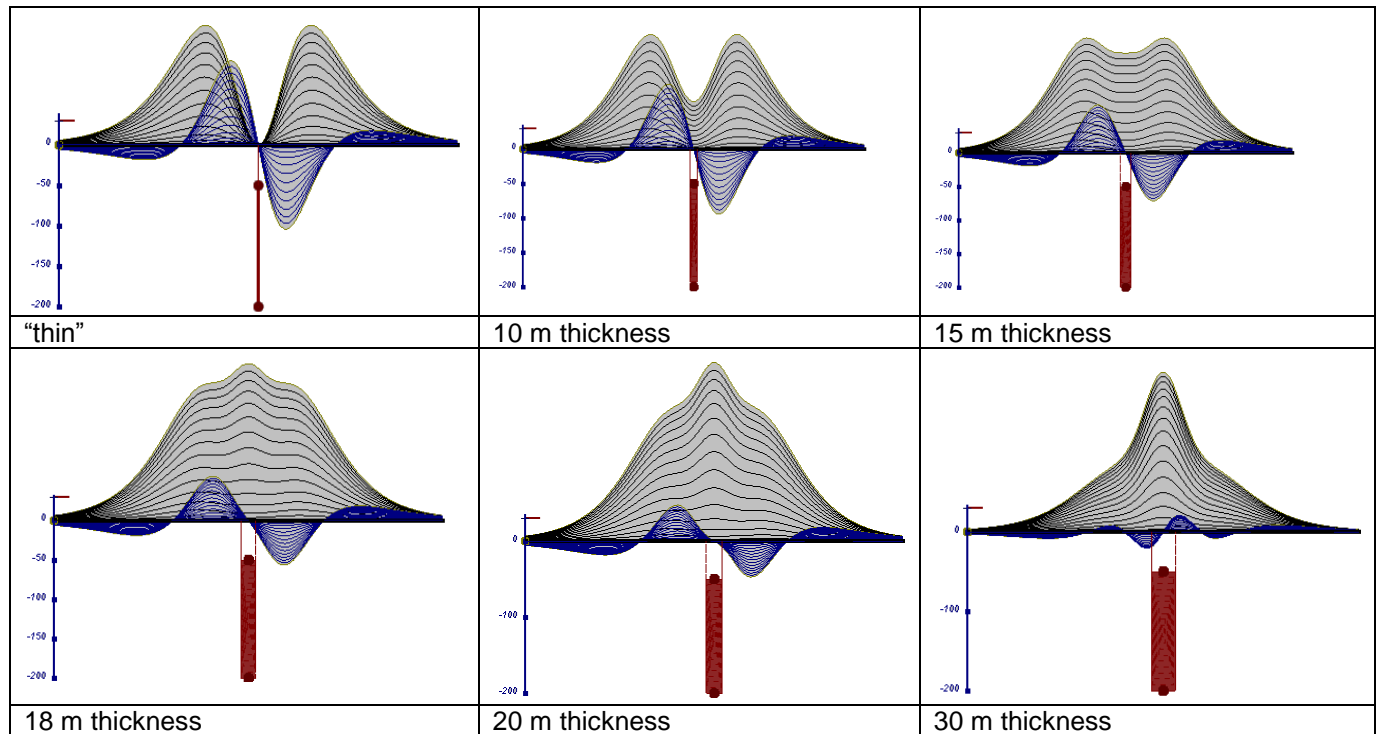


Figure D-16: Conductive vertical plate, depth 50 m, strike length 200 m, depth extends 150 m.

Alexander Prikhodko, PhD, P.Geo
Geotech Ltd.

September 2010

APPENDIX E

EM TIME CONSTANT (TAU) ANALYSIS

Estimation of time constant parameter¹ in transient electromagnetic method is one of the steps toward the extraction of the information about conductances beneath the surface from TEM measurements.

The most reliable method to discriminate or rank conductors from overburden, background or one and other is by calculating the EM field decay time constant (TAU parameter), which directly depends on conductance despite their depth and accordingly amplitude of the response.

Theory

As established in electromagnetic theory, the magnitude of the electro-motive force (emf) induced is proportional to the time rate of change of primary magnetic field at the conductor. This emf causes eddy currents to flow in the conductor with a characteristic transient decay, whose Time Constant (Tau) is a function of the conductance of the survey target or conductivity and geometry (including dimensions) of the target. The decaying currents generate a proportional secondary magnetic field, the time rate of change of which is measured by the receiver coil as induced voltage during the Off time.

The receiver coil output voltage (e_0) is proportional to the time rate of change of the secondary magnetic field and has the form,

$$e_0 \propto (1 / \tau) e^{-(t / \tau)}$$

Where,

$\tau = L/R$ is the characteristic time constant of the target (TAU)

R = resistance

L = inductance

From the expression, conductive targets that have small value of resistance and hence large value of τ yield signals with small initial amplitude that decays relatively slowly with progress of time. Conversely, signals from poorly conducting targets that have large resistance value and small τ , have high initial amplitude but decay rapidly with time¹ (Fig. E1).

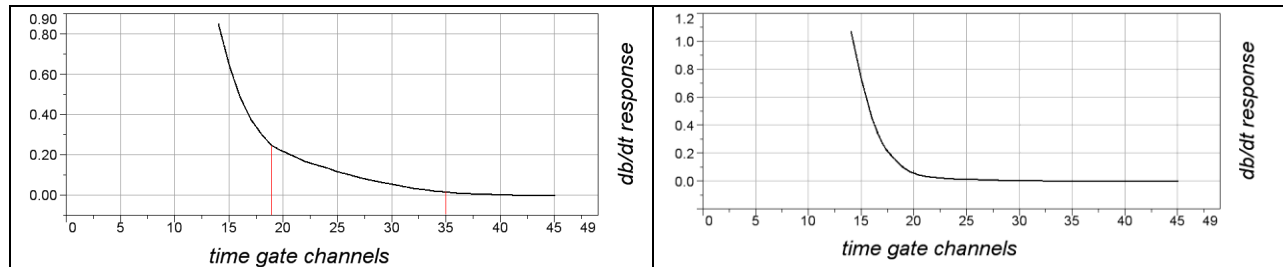


Figure E-1: Left – presence of good conductor, right – poor conductor.

¹ McNeill, JD, 1980, "Applications of Transient Electromagnetic Techniques", Technical Note TN-7 page 5, Geonics Limited, Mississauga, Ontario.

EM Time Constant (Tau) Calculation

The EM Time-Constant (TAU) is a general measure of the speed of decay of the electromagnetic response and indicates the presence of eddy currents in conductive sources as well as reflecting the “conductance quality” of a source. Although TAU can be calculated using either the measured dB/dt decay or the calculated B-field decay, dB/dt is commonly preferred due to better stability (S/N) relating to signal noise. Generally, TAU calculated on base of early time response reflects both near surface overburden and poor conductors whereas, in the late ranges of time, deep and more conductive sources, respectively. For example early time TAU distribution in an area that indicates conductive overburden is shown in Figure 2.

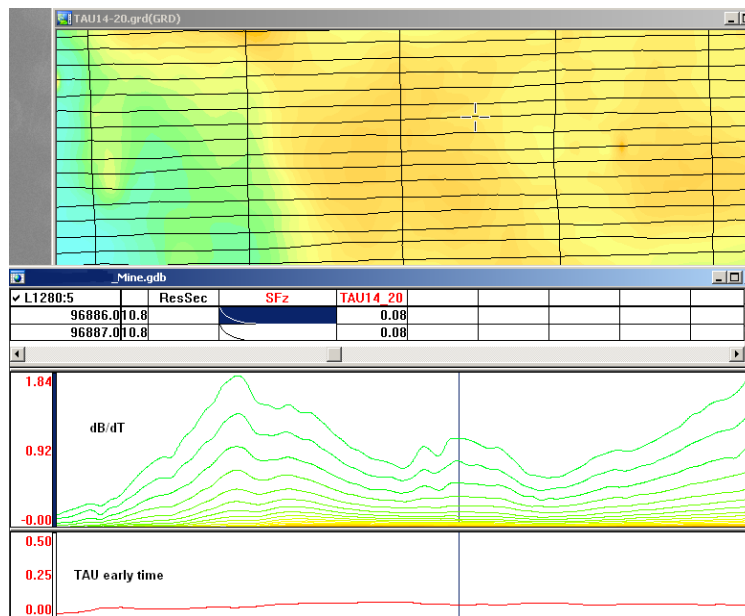


Figure E-2: Map of early time TAU. Area with overburden conductive layer and local sources.

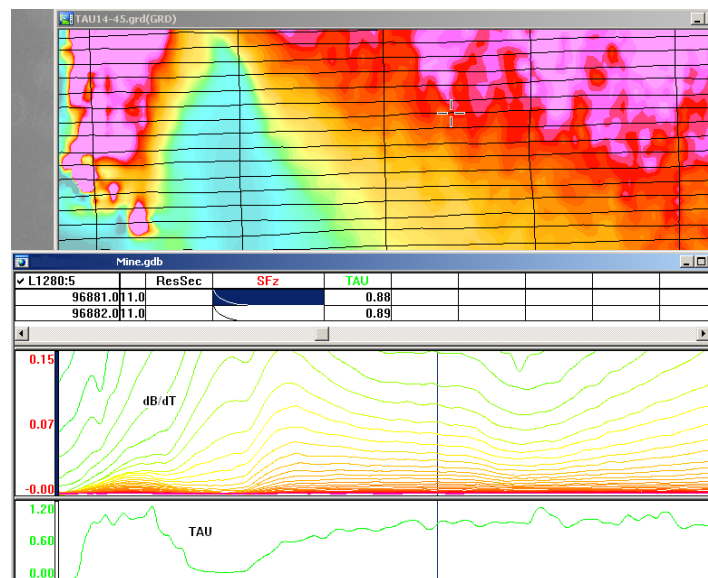


Figure E-3: Map of full time range TAU with EM anomaly due to deep highly conductive target.

There are many advantages of TAU maps:

- TAU depends only on one parameter (conductance) in contrast to response magnitude;
- TAU is integral parameter, which covers time range and all conductive zones and targets are displayed independently of their depth and conductivity on a single map.
- Very good differential resolution in complex conductive places with many sources with different conductivity.
- Signs of the presence of good conductive targets are amplified and emphasized independently of their depth and level of response accordingly.

In the example shown in Figure 4 and 5, three local targets are defined, each of them with a different depth of burial, as indicated on the resistivity depth image (RDI). All are very good conductors but the deeper target (number 2) has a relatively weak dB/dt signal yet also features the strongest total TAU (Figure 4). This example highlights the benefit of TAU analysis in terms of an additional target discrimination tool.

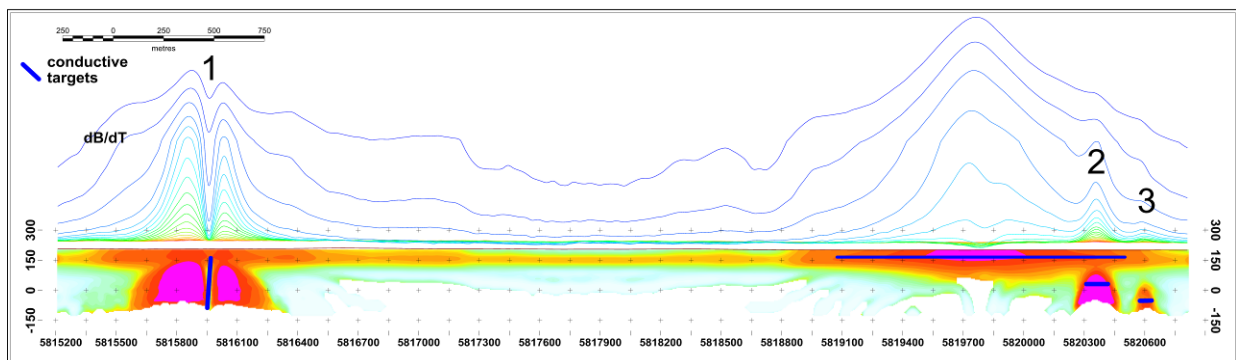


Figure E-4: dB/dt profile and RDI with different depths of targets.

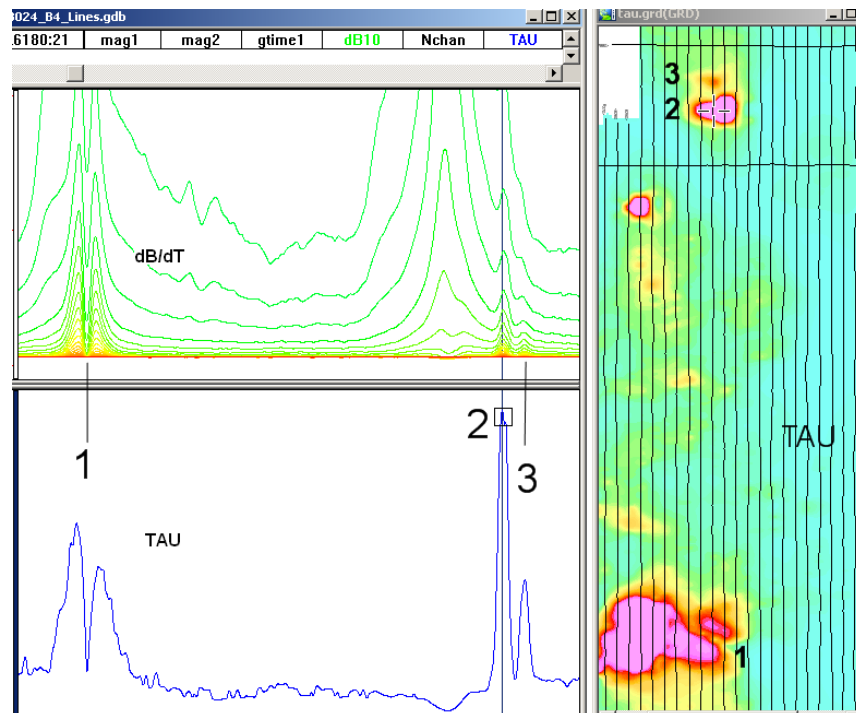


Figure E-5: Map of total TAU and dB/dt profile.

The EM Time Constants for dB/dt and B-field were calculated using the “sliding Tau” in-house program developed at Geotech2. The principle of the calculation is based on using of time window (4 time channels) which is sliding along the curve decay and looking for latest time channels which have a response above the level of noise and decay. The EM decays are obtained from all available decay channels, starting at the latest channel. Time constants are taken from a least square fit of a straight-line (log/linear space) over the last 4 gates above a pre-set signal threshold level (Figure F6). Threshold settings are pointed in the “label” property of TAU database channels. The sliding Tau method determines that, as the amplitudes increase, the time-constant is taken at progressively later times in the EM decay. Conversely, as the amplitudes decrease, Tau is taken at progressively earlier times in the decay. If the maximum signal amplitude falls below the threshold, or becomes negative for any of the 4 time gates, then Tau is not calculated and is assigned a value of “dummy” by default.

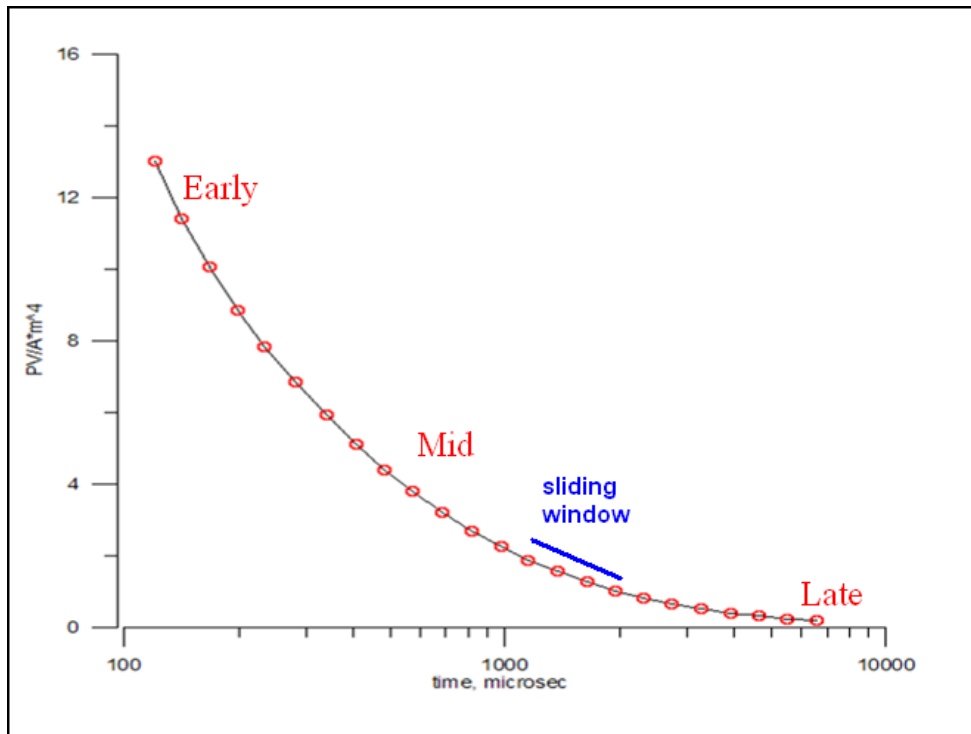


Figure E-6: Typical dB/dt decays of Vtem data

Alexander Prikhodko, PhD, P.Ge
Geotech Ltd.

September 2010

² by A.Prikhodko

APPENDIX F

TEM RESISTIVITY DEPTH IMAGING (RDI)

Resistivity depth imaging (RDI) is a technique used to rapidly convert EM profile decay data into an equivalent resistivity versus depth cross-section, by deconvolving the measured TEM data. The used RDI algorithm of Resistivity-Depth transformation is based on the scheme of the apparent resistivity transform of Maxwell A. Meju (1998)¹ and TEM response from a conductive half-space. The program is developed by Alexander Prikhodko and is depth-calibrated based on forward plate modeling for VTEM system configuration (Fig. 1-10).

RDIs provide reasonable indications of conductor relative depth and vertical extent, as well as accurate 1D layered-earth apparent conductivity/resistivity structure across VTEM flight lines. Approximate depth of investigation of a TEM system, image of secondary field distribution in half-space, effective resistivity, initial geometry and position of conductive targets is the information obtained on the basis of the RDIs.

Maxwell forward modeling with RDI sections from the synthetic responses (VTEM system)

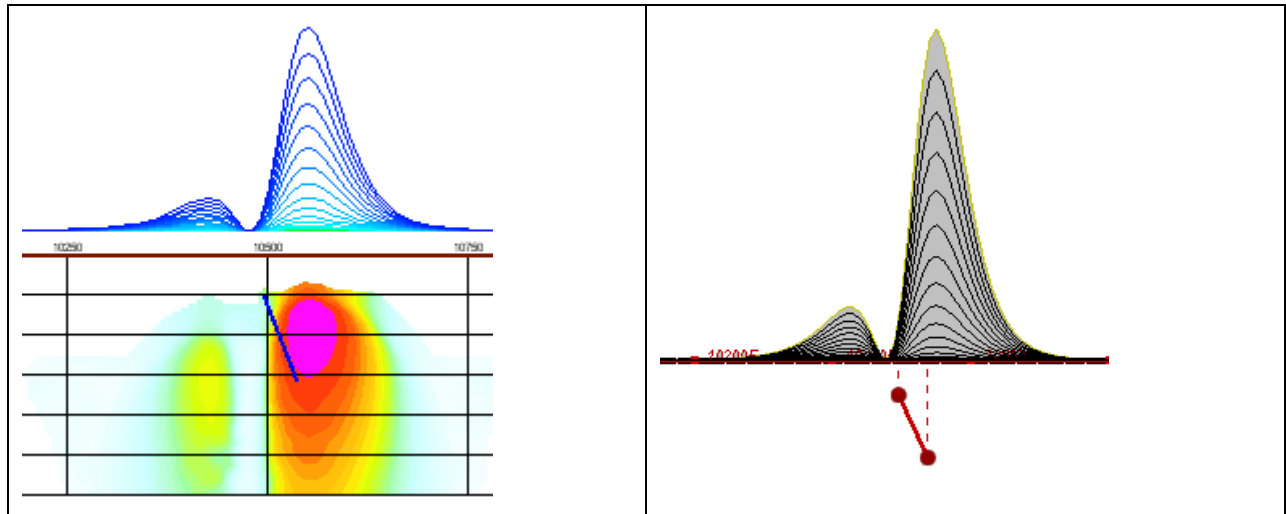


Figure F-1: Maxwell plate model and RDI from the calculated response for a conductive “thin” plate (depth 50 m, dip 65 degree, depth extend 100 m).

¹ Maxwell A. Meju, 1998, Short Note: A simple method of transient electromagnetic data analysis, *Geophysics*, **63**, 405–410.

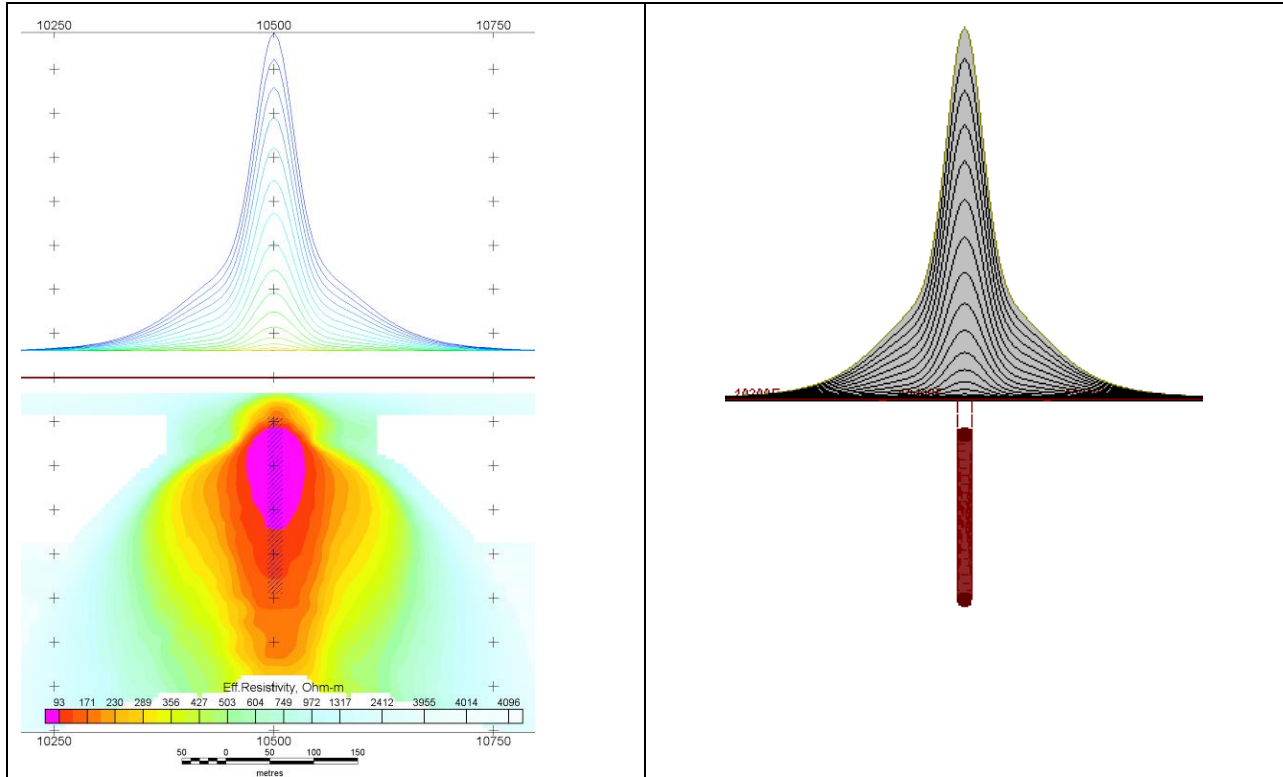


Figure F-2: Maxwell plate model and RDI from the calculated response for “thick” plate 18 m thickness, depth 50 m, depth extend 200 m).

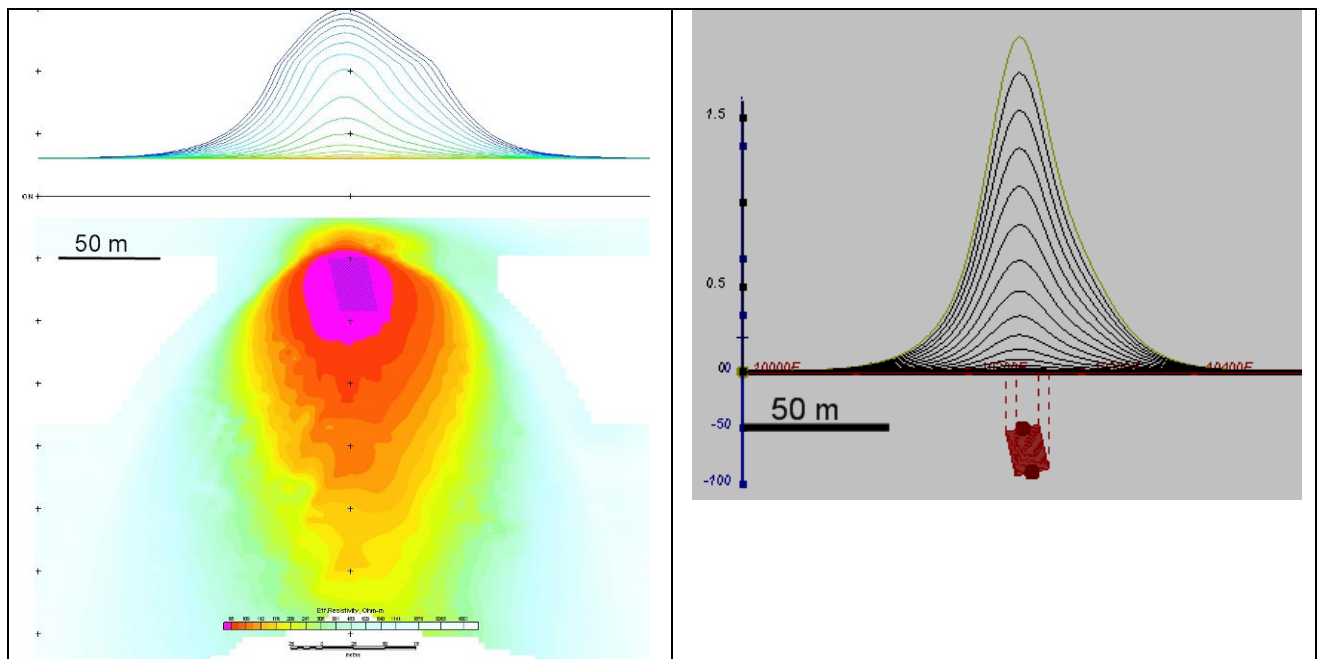


Figure F-3: Maxwell plate model and RDI from the calculated response for bulk (“thick”) 100 m length, 40 m depth extend, 30 m thickness

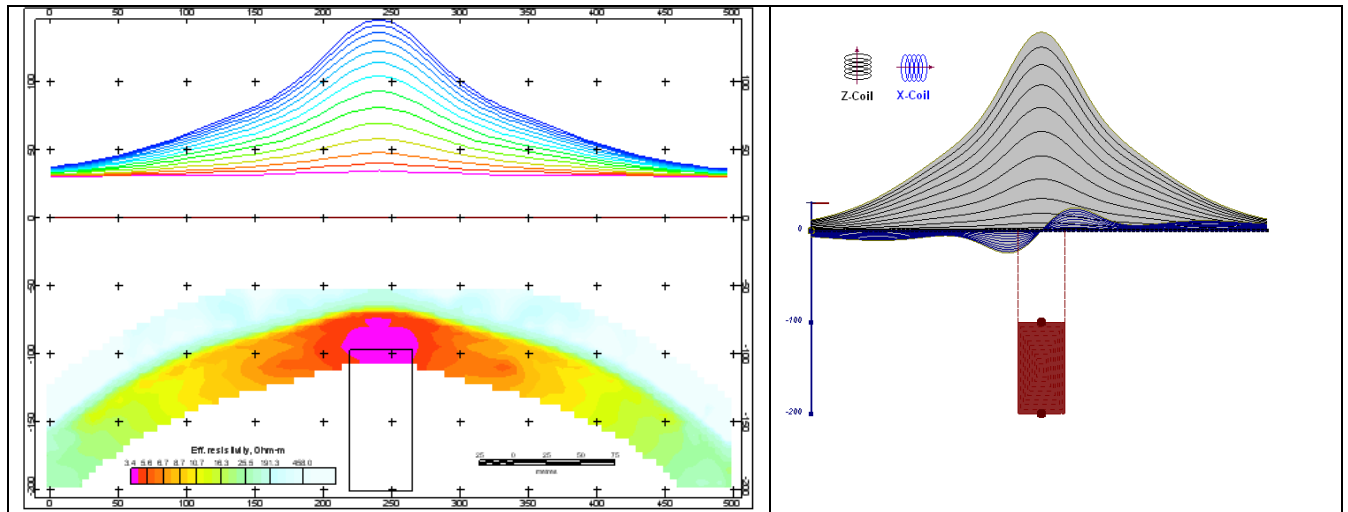


Figure F-4: Maxwell plate model and RDI from the calculated response for “thick” vertical target (depth 100 m, depth extend 100 m). 19-44 chan.

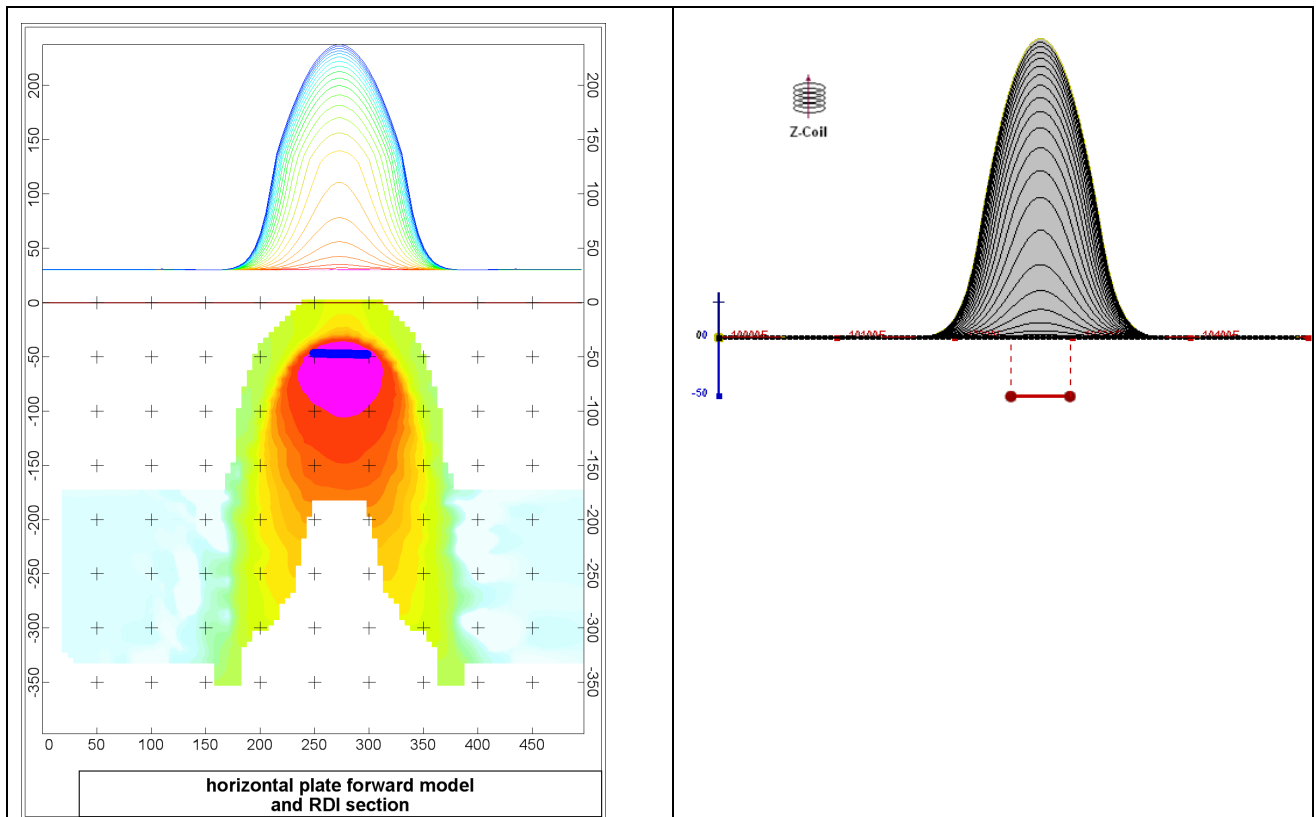


Figure F-5: Maxwell plate model and RDI from the calculated response for horizontal thin plate (depth 50 m, dim 50x100 m). 15-44 chan.

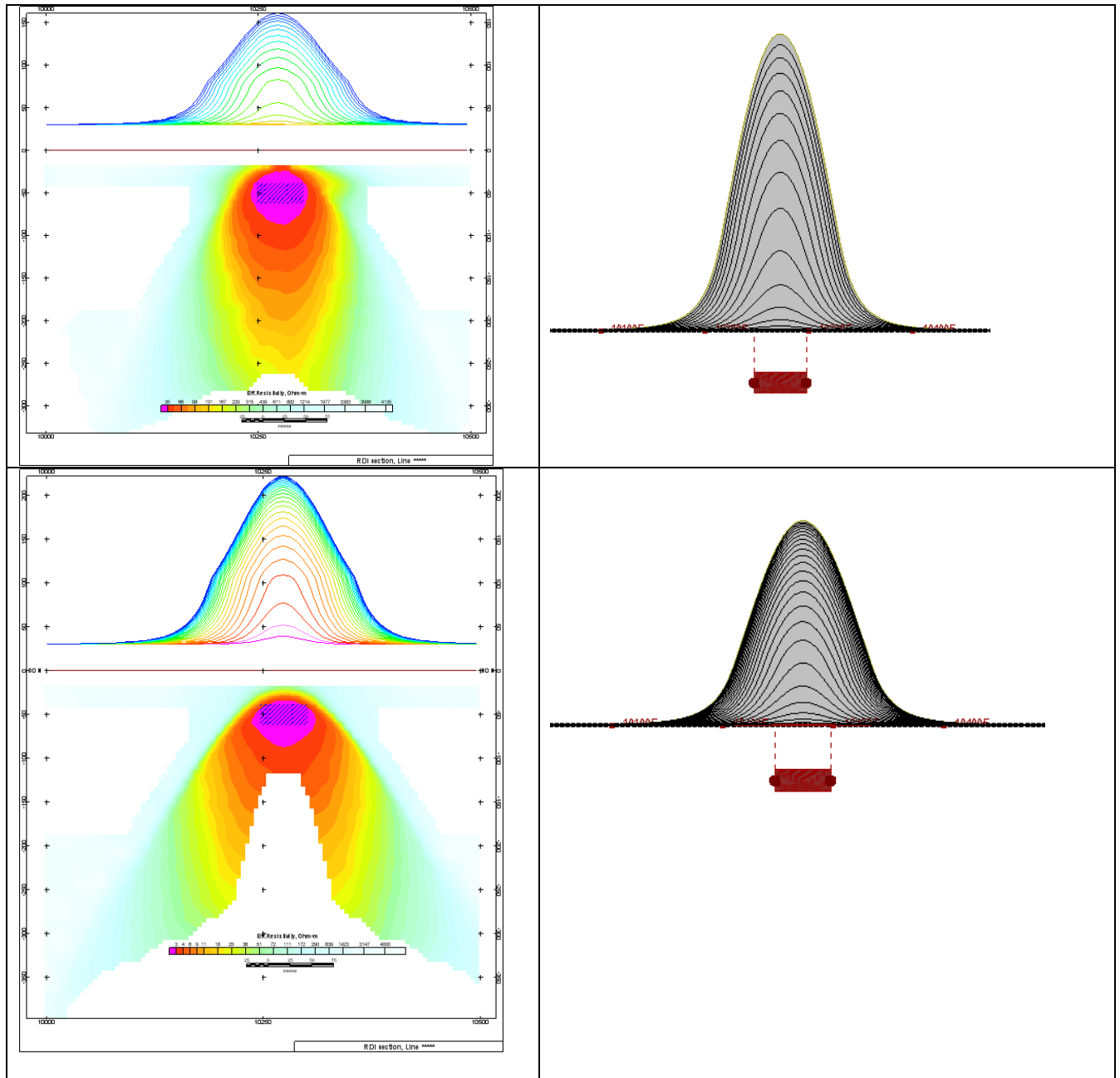


Figure F-6: Maxwell plate model and RDI from the calculated response for horizontal thick (20m) plate – less conductive (on the top), more conductive (below)

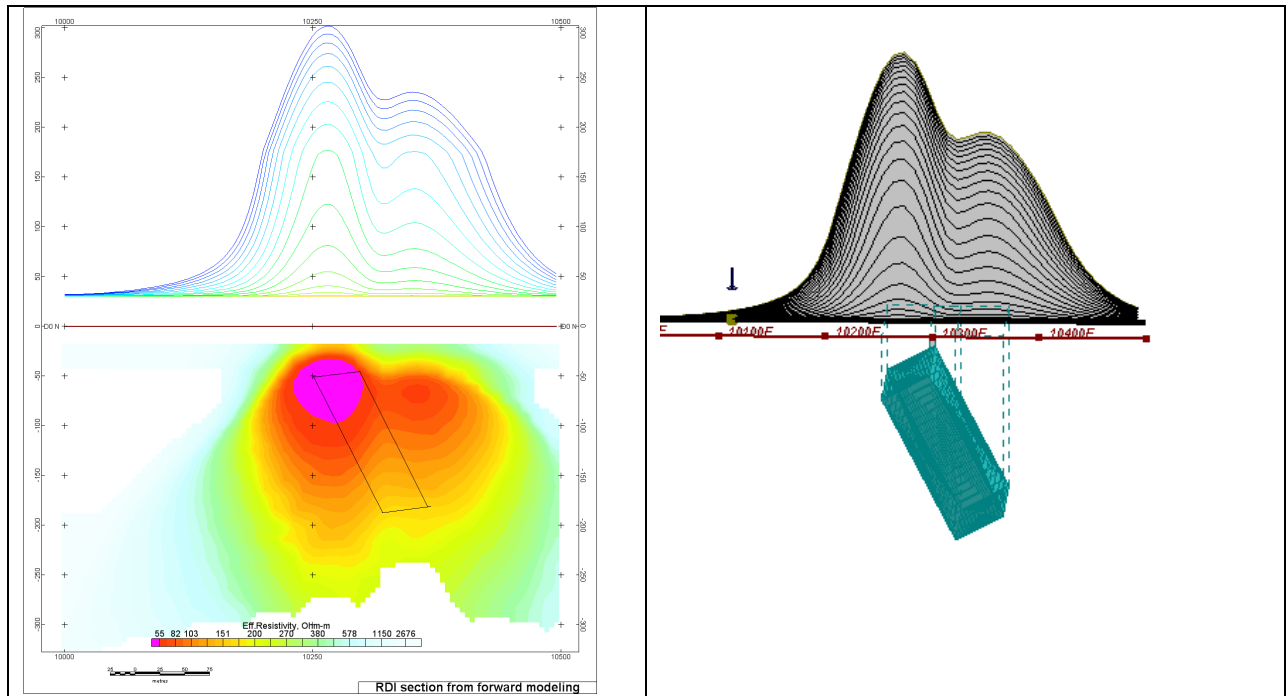


Figure F-7: Maxwell plate model and RDI from the calculated response for inclined thick (50m) plate. Depth extends 150 m, depth to the target 50 m.

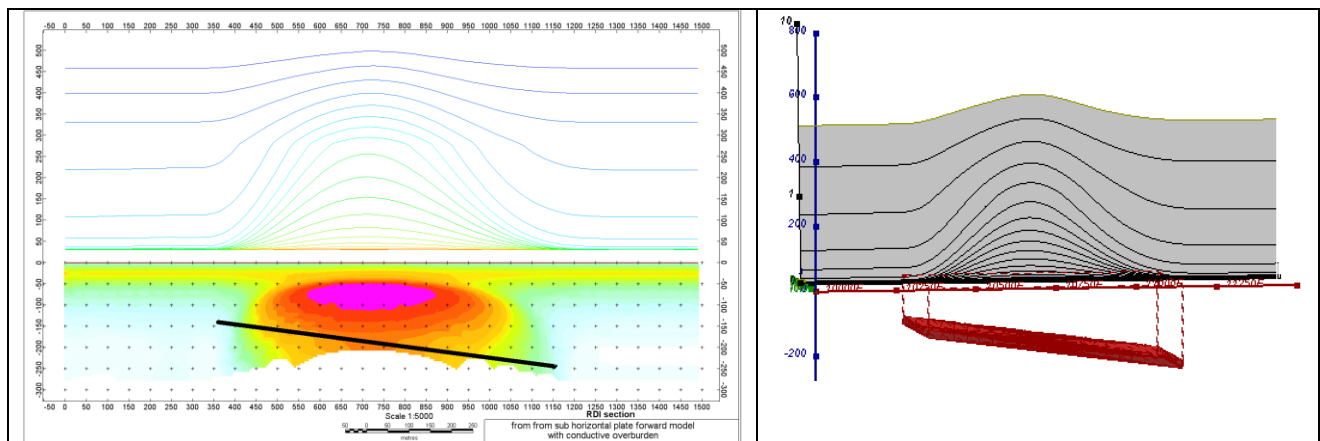


Figure F-8: Maxwell plate model and RDI from the calculated response for the long, wide and deep subhorizontal plate (depth 140 m, dim 25x500x800 m) with conductive overburden.

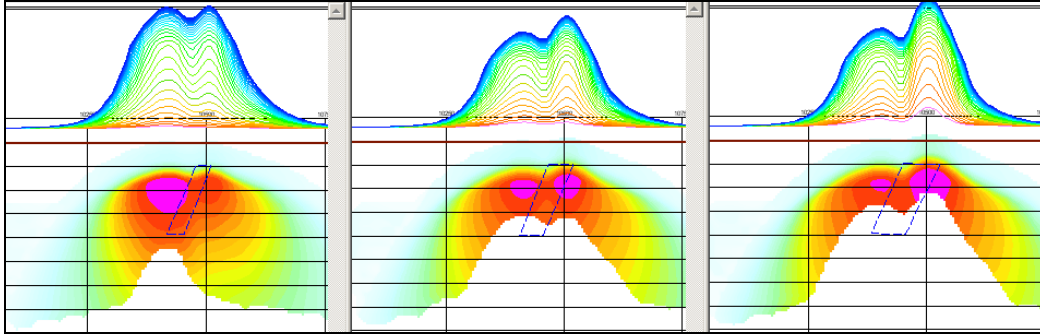


Figure F-9: Maxwell plate models and RDIs from the calculated response for “thick” dipping plates (35, 50, 75 m thickness), depth 50 m, conductivity 2.5 S/m.

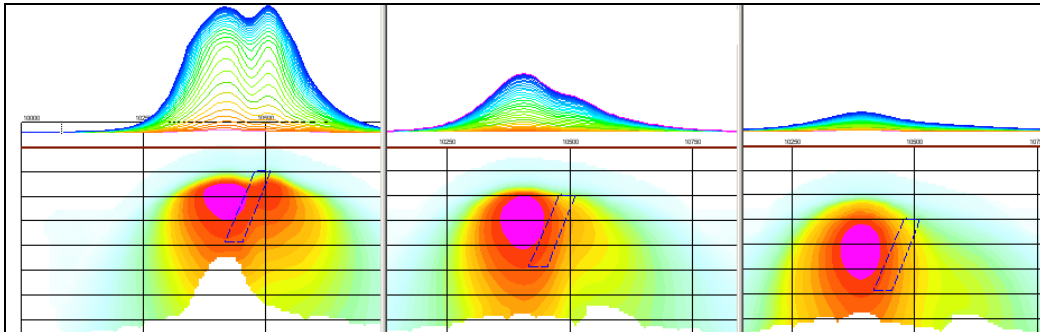


Figure F-10: Maxwell plate models and RDIs from the calculated response for “thick” (35 m thickness) dipping plate on different depth (50, 100, 150 m), conductivity 2.5 S/m.

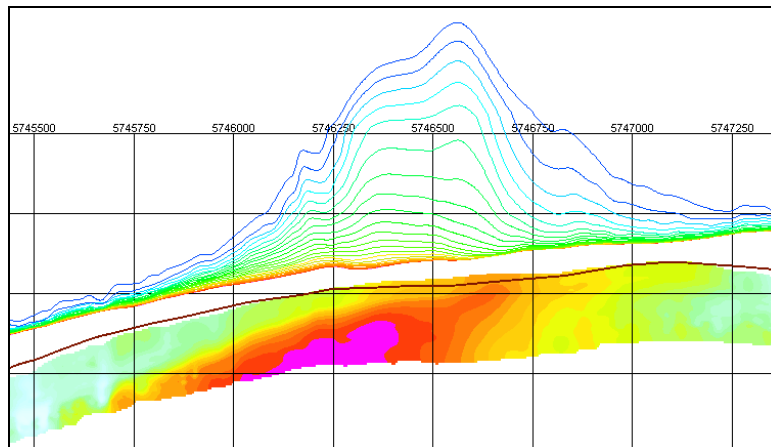
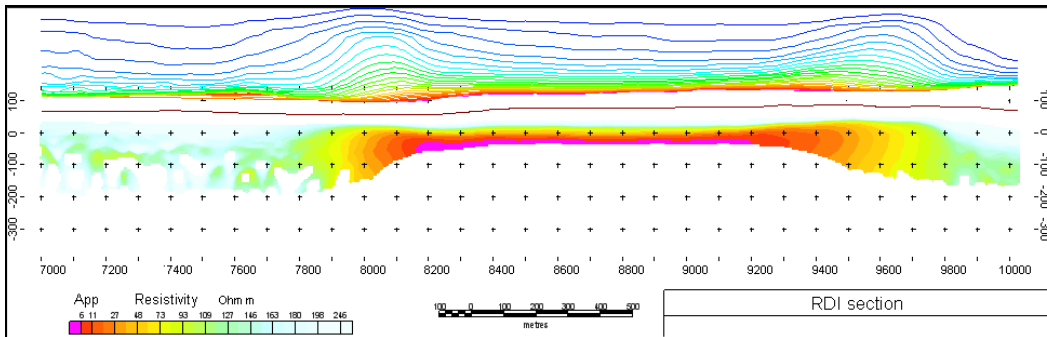
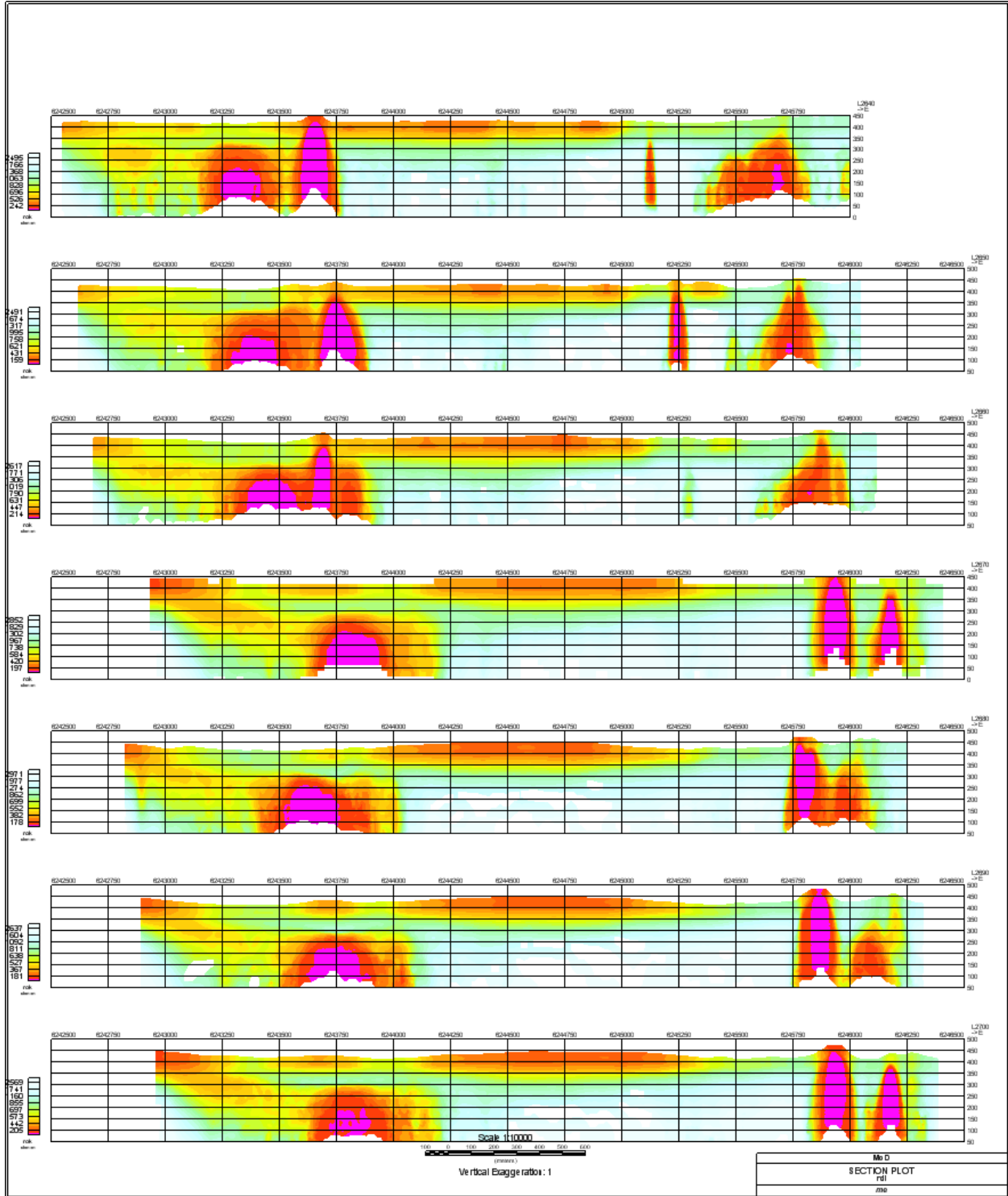


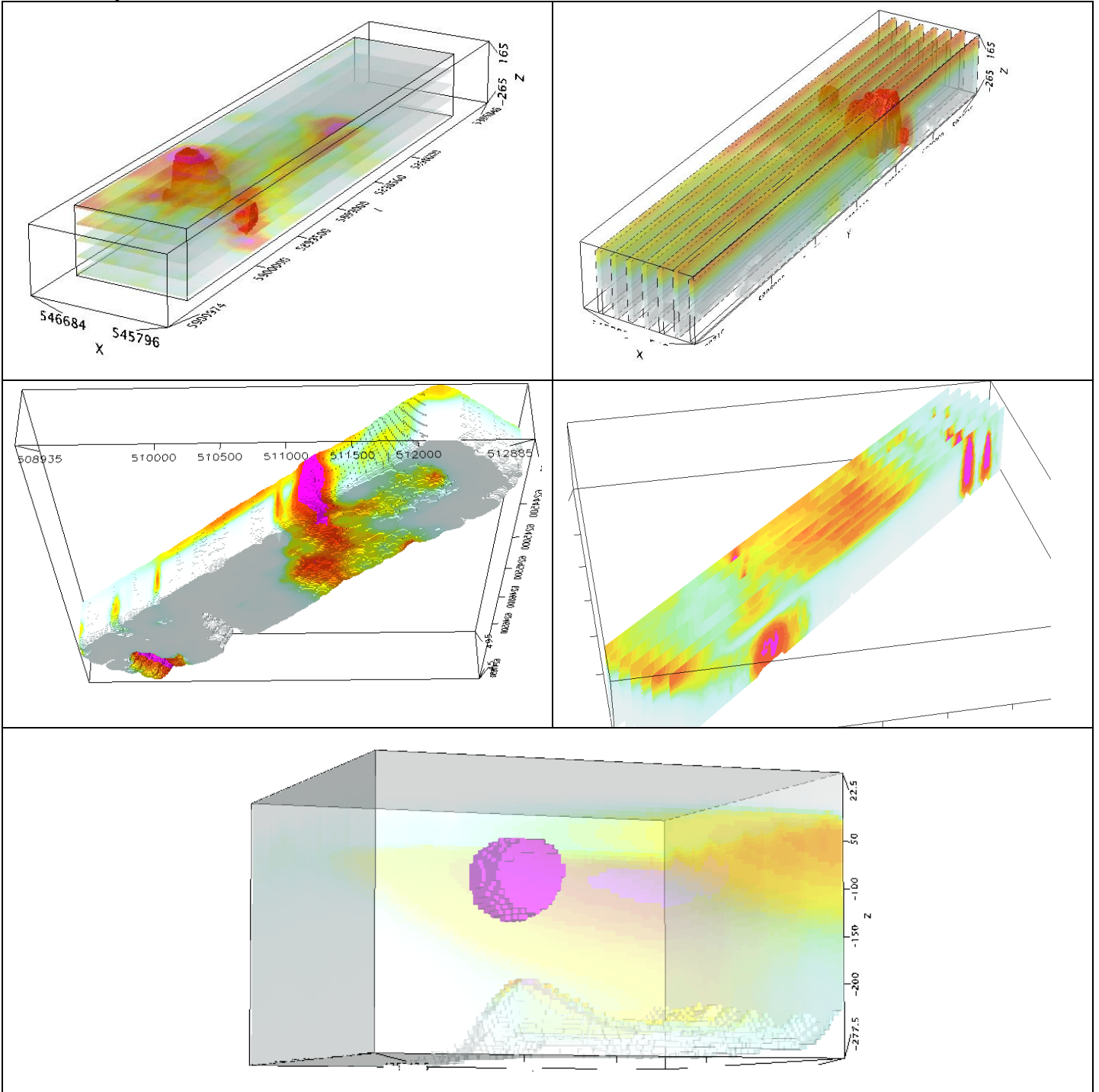
Figure F-11: RDI section for the real horizontal and slightly dipping conductive layers

FORMS OF RDI PRESENTATION

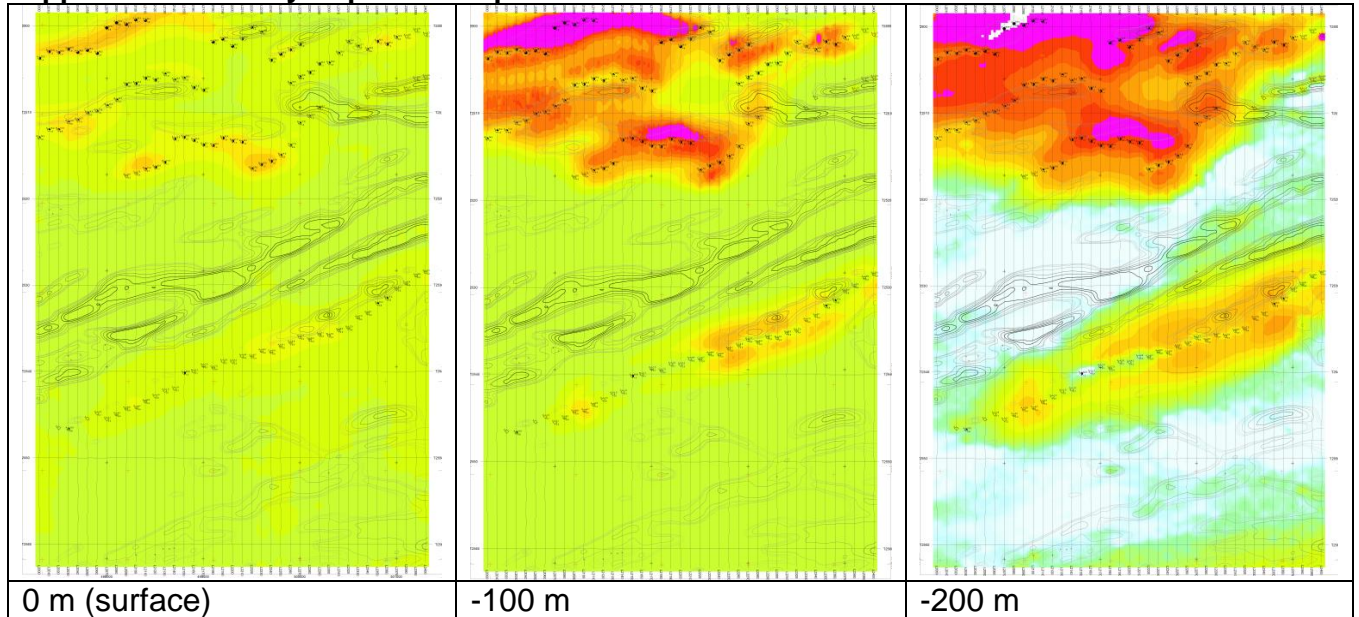
Presentation of series of lines



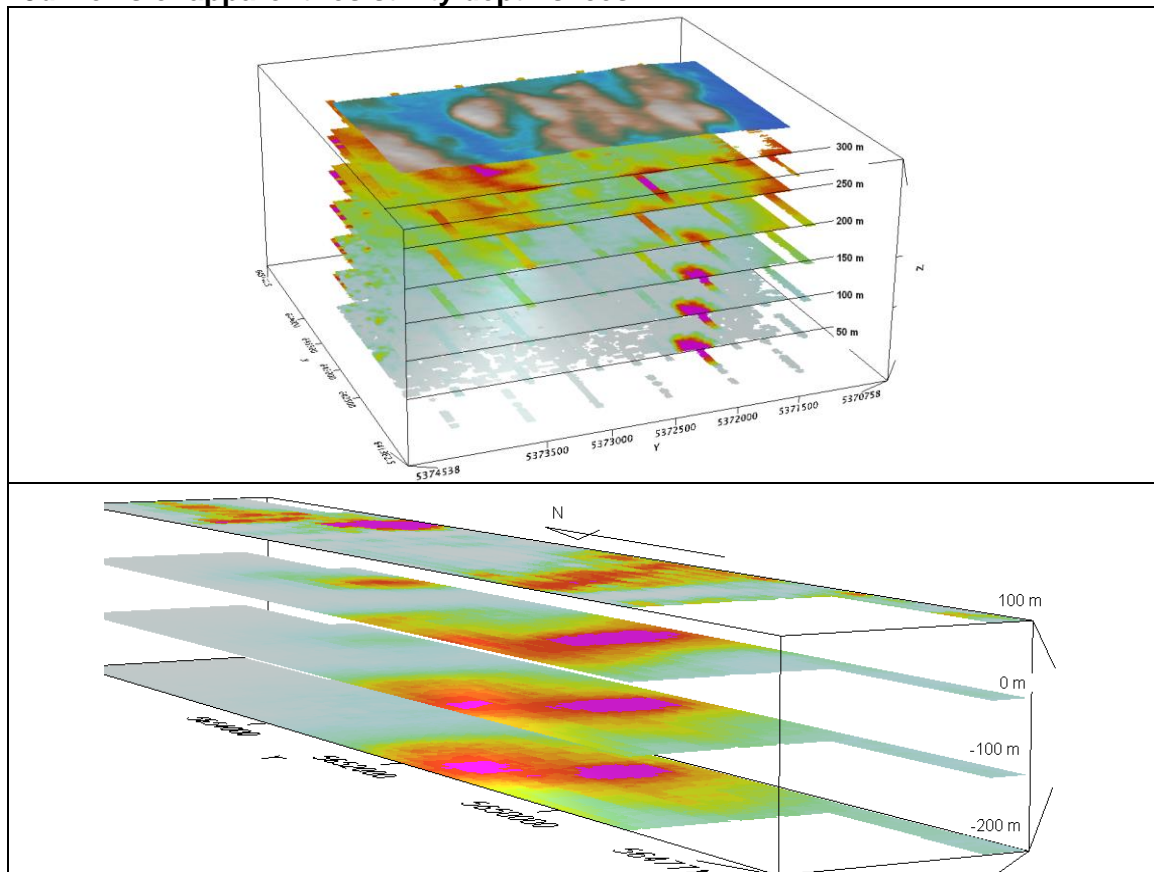
3d presentation of RDIs



Apparent Resistivity Depth Slices plans:

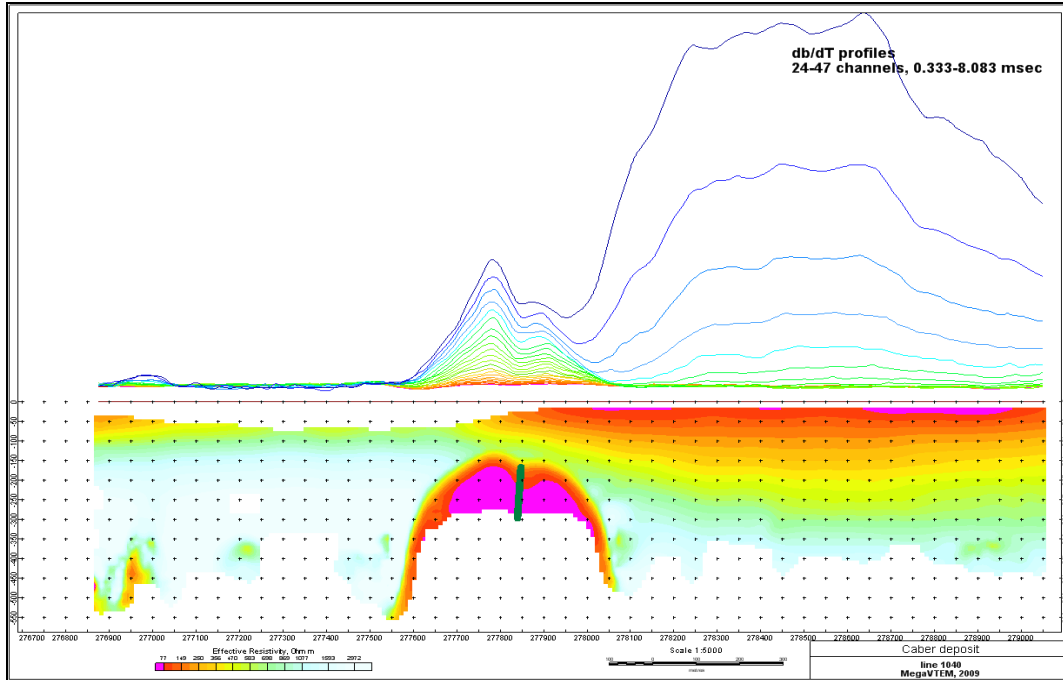


3d views of apparent resistivity depth slices:

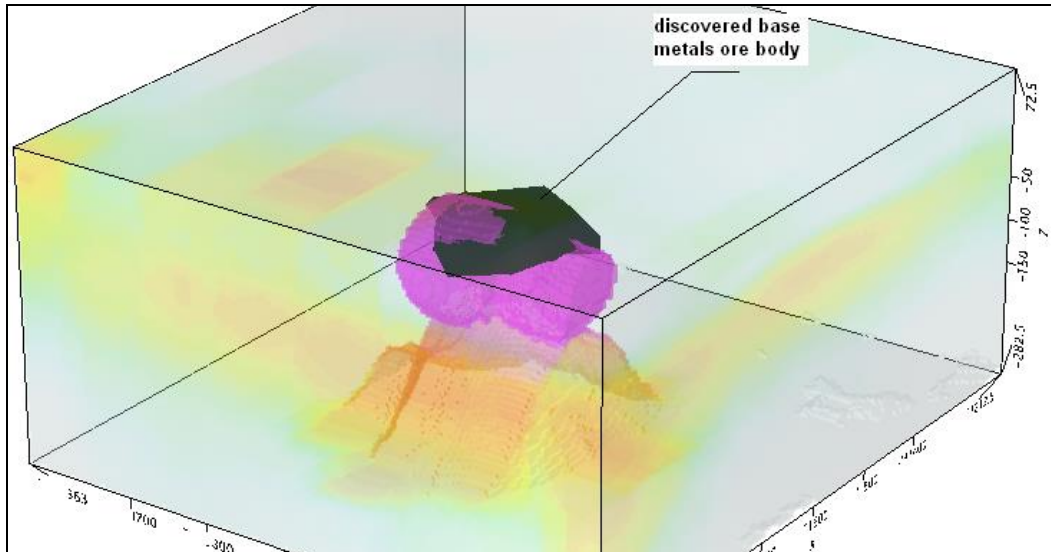


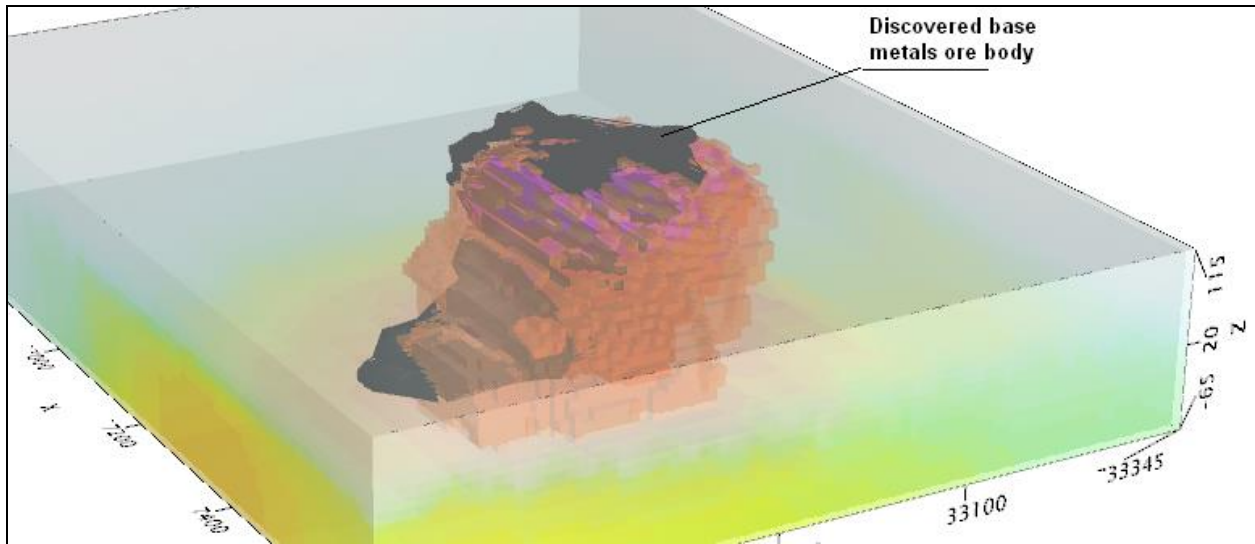
Real base metal targets in comparison with RDIs:

RDI section of the line over Caber deposit ("thin" subvertical plate target and conductive overburden).



3d RDI voxels with base metals ore bodies (Middle East):





Alexander Prikhodko, PhD, P.Geo
Geotech Ltd.
April 2011